# WISE - USER GUIDE AND IMPLEMENTATION NOTES

P. Hagen, CERN, Geneva, Switzerland

## ABSTRACT

The goal of WISE is to prepare an "accurate as possible" description of the LHC magnetic and geometric properties for use by the MAD-X model of the machine. WISE is designed to take into account the best estimate of uncertainties. The reason being that magnetic and geometric measurements have error bars associated with them, like calibration and resolution. Therefore WISE produces a number of instances of the most likely LHC machine that may be used to predict ranges of beam parameters. Magnetic and geometric data are downloaded from the different databases, missing information is completed, and uncertainties are added. This report contains a short section on how using the code and a detailed description of how data relative to magnetic and geometric imperfections, and slot allocation are prepared. The code is built as a transparent box, thus allowing inspection of all the information acquired during the production and test of the LHC magnets. The user interface offers a range of options that allow testing of hypothesis and assigning imperfections to subsets of the machine.

## TABLE OF CONTENTS

## 1. INTRODUCTION

The simulation tool "Windows Interface to Simulation of Errors" (WISE) is a pre-processor for MAD-X [1]. It generates files with magnetic field imperfections estimated on the basis of magnetic measurements and slot allocation, as well as tables with geometric misalignments that can be used as input files for MAD-X. In addition, template scripts are provided to run MAD-X with perturbed optics. Most parts of the software code are of general nature, although numerous tables and embedded data inside WISE are specific for the LHC optics [2]. Fig.1 shows a simplified diagram of data inputs, processing and output.

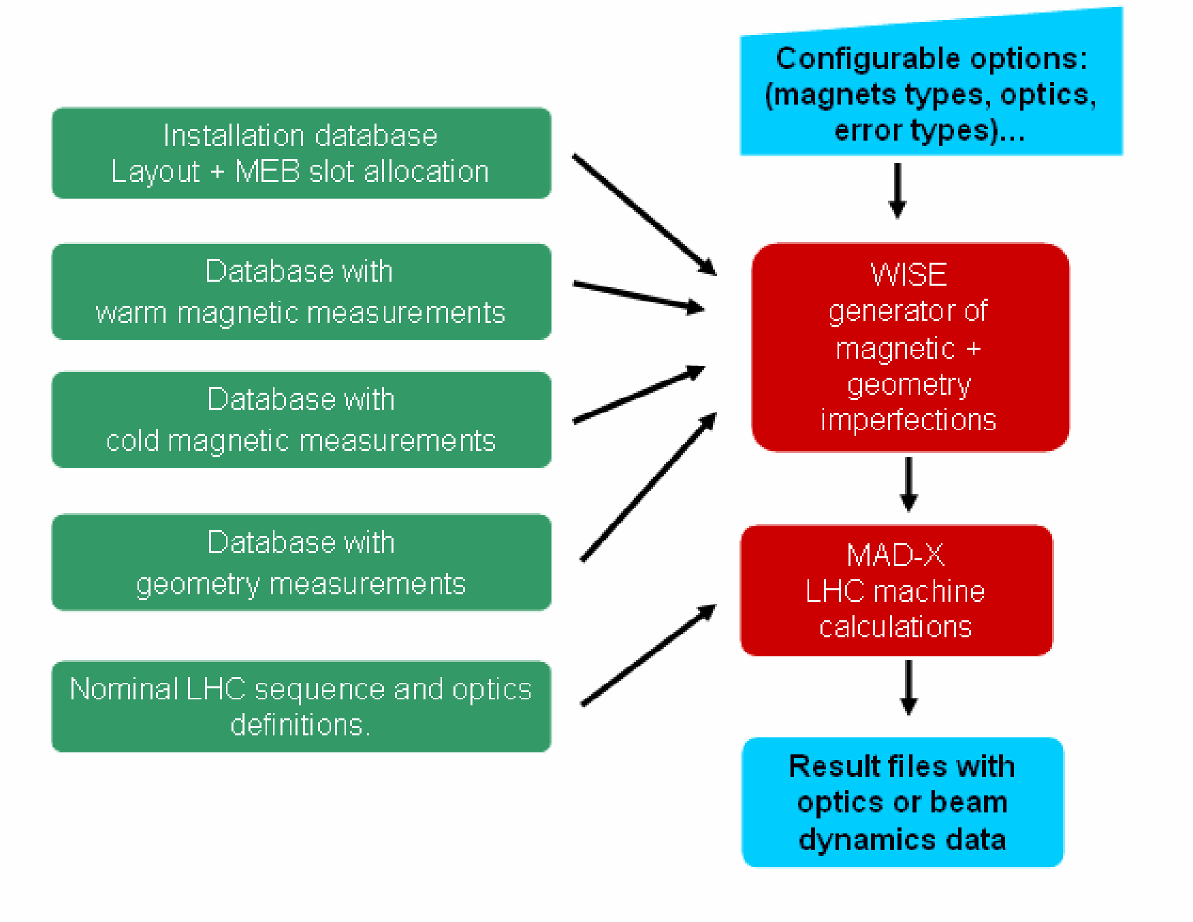


Fig. 1. Processing flow in *Wise.xls*.

The WISE tool has been implemented as Visual Basic code inside Excel to allow a quick implementation and debugging. Spreadsheets allow the code to be data driven, making it easier for data validation as the results from intermediate calculations can be read and analysed. The trade-off is that the code is mainly interactive and therefore ill-suited for integration into a server application. However, it was felt that the first priority is to quickly produce a validated simulation, leaving to a second phase a more mature implementation software-wise, based upon usage feedback and future requirements.

The aim of this report is to inform the user of WISE about what it can and cannot do, along with anecdotes about internal algorithms and known trade-offs. This report is divided into two major parts. Section 2 shows how to use WISE. Sections 3 to 5 describe the implementation. Some background material is covered in appendices.

## 2. HOW TO RUN A SIMULATION

It is assumed that you already have installed the software on your Windows PC, following the guidelines given in appendix A. This section focuses on the usage without entering into background or implementation details.

Start WISE by opening the workbook *Wise.xls*. Activate the *enable macro* option. It contains many worksheets that will be described later in this report. You will find a *Simulation* menu with several sub options. Click on *Run Simulation* (see Fig. 2.)

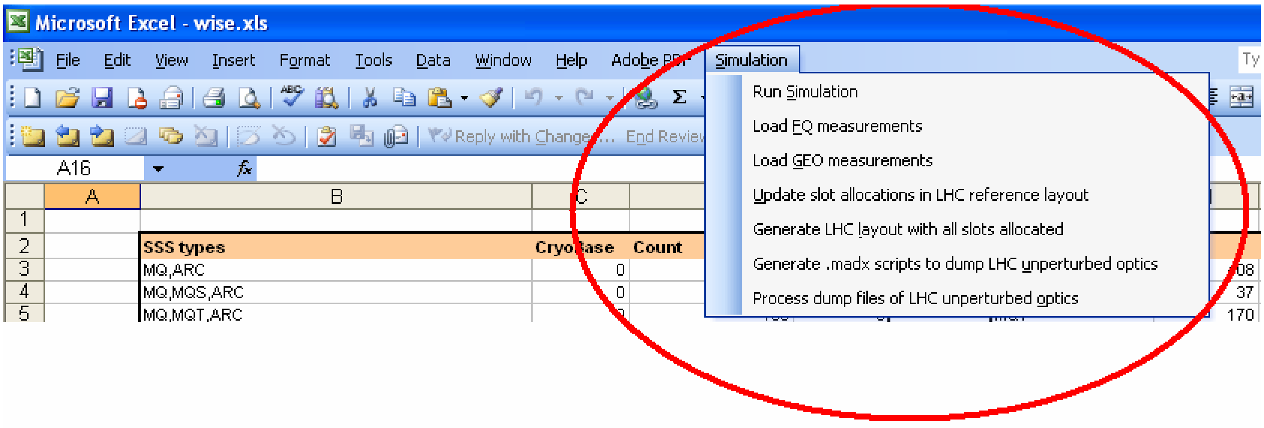


Fig. 2. The *Simulation* menu in *Wise.xls*.

### 2.1 Main simulation form

The main simulation form (Fig. 3) allows you to select what to simulate and the major boundary conditions. More subtle options are sometimes needed and can be accessed by clicking the *Options* button (see Fig. 4). Positioning the mouse over an option gives a short "tool-tip". Choices made in the menus are remembered for subsequent usage. They are stored in the sheet *GUI*. In addition to these menus, it is possible to manipulate numerous tables in the *Summary* worksheet. One of the goals of the WISE software is to make it data-driven such that it can be made more complete (more tables) and more accurate (updates of existing figures) over time.

The main simulation form (Fig. 3) has many choices which are grouped together in "frames".

- *Simulation name* is the name prefix used to generate the output files from WISE. It is recommended to use a name that characterises the simulation. Do not include special characters like spaces as the files need to be copied to the UNIX platform. Later in this section (section 2.4) we will describe what files are generated by WISE.

- *Iterations* is the number of times you want to repeat the simulation. Executing more than one simulation only makes sense if random generators are used, either to simulate uncertainties in the measurements, or in the slot allocation. In this case several instances of the machine are created.

- *Iterations before new slot allocation* allows to keep the same slot allocation (draw of empty slots in the LHC machine) for several simulations. Example: You choose 30 iterations and to make a new draw for each 5 iteration. You are then simulating 6=30/5 different lay-outs, each one with 5 generations of uncertainties. The implementation of the slot allocation is discussed in section 5.

* *Output folder* is the local PC Windows folder where WISE writes all the output files.

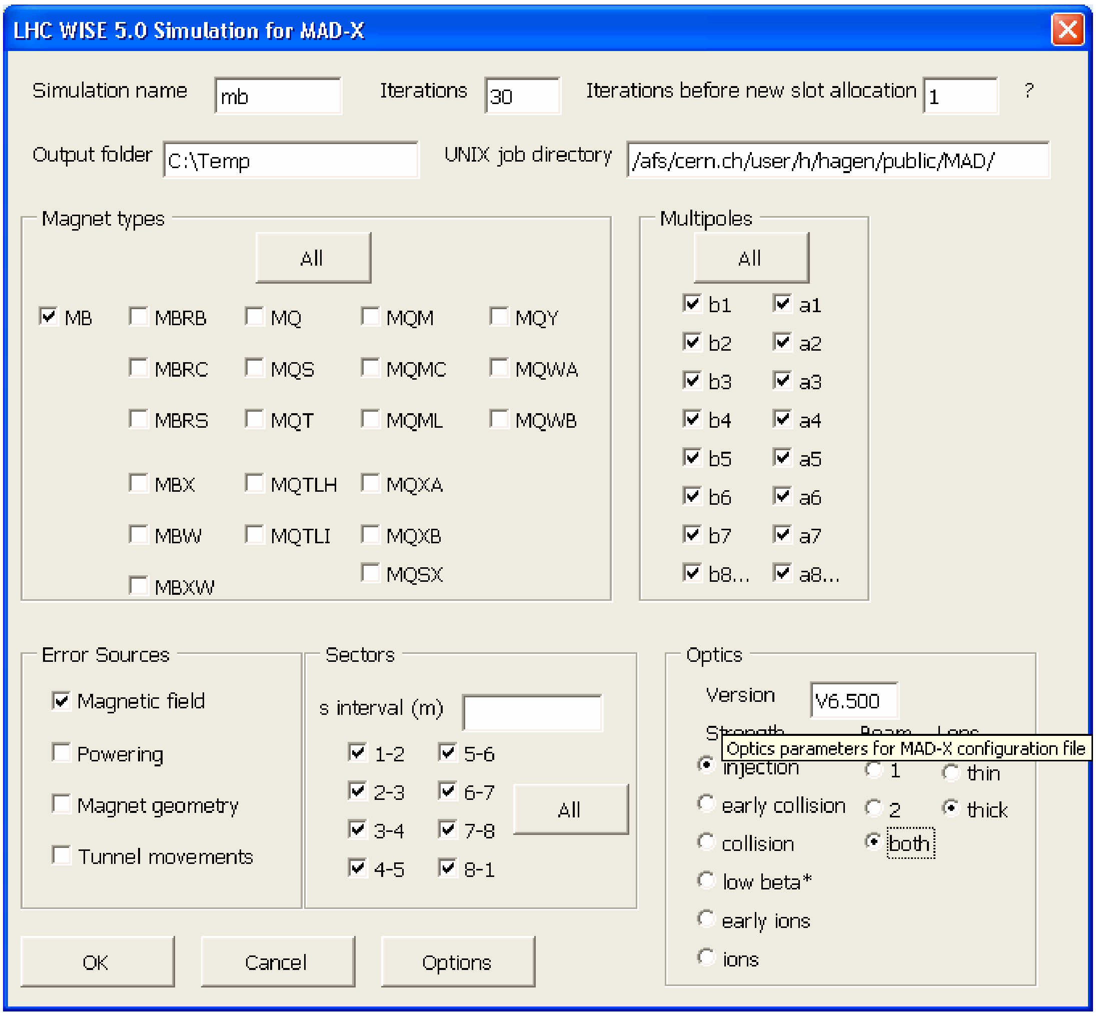


Fig. 3. The main *Simulation* form in *Wise.xls*.

* *UNIX job directory is* the remote UNIX directory where MAD-X will be run. The reason for this parameter is that these directories are necessary for writing MAD-X script files.

* *Magnet Types* are the magnets whose imperfections can be selected (one or more). It contains the main magnets and a selection of correctors.

* *Error Sources* are the driving sources of imperfections.

    o *Magnetic field* generates main field and multipole errors for the given magnet types based on the best knowledge according to measurements

    o *Powering* generates the errors stemming from power supply (i.e., uncertainties in the main field given by the magnet, see section 3).

    o *Magnet geometry* generates alignment errors due to imperfections in the shape of the magnets (see section 4).

    o *Tunnel movements* generate alignment errors due to errors in the cryostat position in the tunnel, and its movements over time (see section 4). In this case, errors are generated for all magnets inside a cryostat having at least one of the selected magnet types.

- *Multipoles* are which field multipoles we want to generate errors for. This choice is only relevant for the magnetic field and powering error sources.

- *Sectors* allow you to generate imperfection only for a subset of the machine or s-intervals in LHC clockwise direction. It is sometimes of interest to see error contributions from a small fraction of the whole machine.

- *Optics* is for MAD-X specific choices. MAD-X needs to know what state (strength), beam and model (lens type) we want to use (see appendix B).

### 2.2 Options simulation form

We now briefly describe the *Options* form shown in Fig. 4.

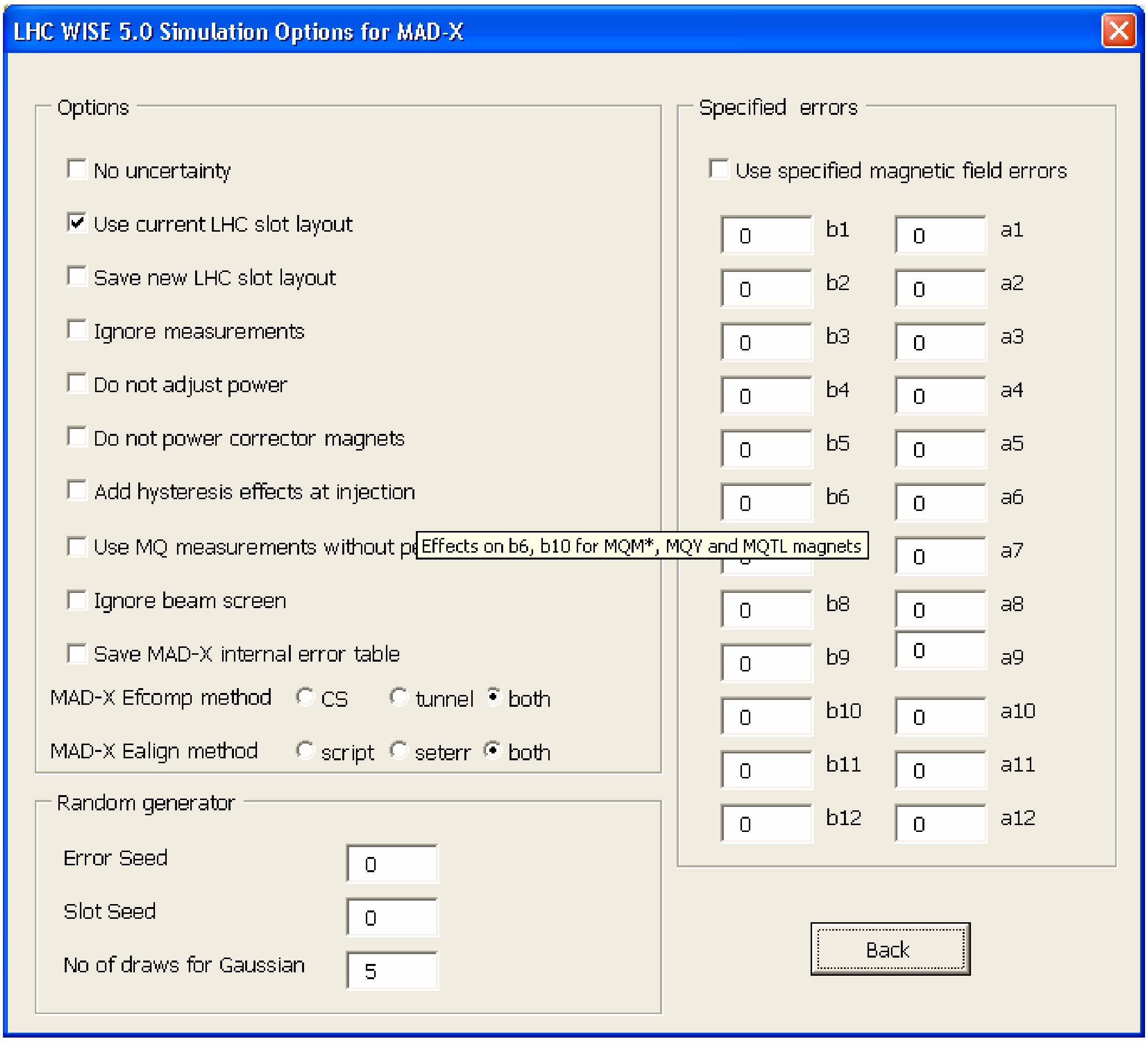


Fig. 4. The *Options* form in *Wise.xls*.

- *No uncertainty* is used to disable random errors that are added to estimate imperfections. Using this option, for instance, warm-cold correlations are considered as a simple deterministic offset, and the estimated errors associated to the measurements system are neglected. In this case, the only variability left in the simulation is the generation of field errors for magnets which are not measured.

- *Use current LHC layout* disables the generation of a new LHC lay-out for slots which are not yet allocated. In this case the lay-out recorded in the worksheet *LHC gen layout* is used. This option overrides the main form option *Iterations before new slot allocation*.

- *Save new LHC slot layout* writes new slot allocations to files (see section 5).

- *Ignore measurements* makes all errors to be generated as random draws of the statistics given in the *Summary* sheet.

- *Do not adjust power* disables the setting to zero of the average of the main field errors associated to same power supply. Example: if this function is not enabled, the average of the errors in the transfer function of dipoles in the same sector is set to zero.

- *Do not power correctors* disables powering of corrector magnets. This option is currently limited to the spool pieces MCS and MCDO inside the main dipoles. Powering of other correctors is assumed to take place outside WISE by implementing correction strategies directly in MAD-X.

- *Add hysteresis effect at injection* enables a model for MQM and MQY which takes into account the variation of the errors with the powering current, based on FiDeL estimates coded inside Wise.

- *Use MQ measurements without permeability correction* allows to use for simulation the raw warm data for the MQ magnets before the correction of permeability (see section 3). Used for what if scenarios, since the corrected data are the best available estimate.

- *Ignore beam screen* does not include the beam screen in the evaluation of the field errors (see section 3).

- *MAD-X Ealign method* is described in section 4.

- *Random generator* is described in appendix C.

- *Specified errors* allows to assign constant multipole errors for the magnetic field error source. That is, no measurements and random draws are involved. Used for what if scenarios, see section 3.

### 2.3 Updating information on worksheets

Measurement data for the magnetic field quality and geometry errors are downloaded from several databases. They are stored in WISE for data validation, inspection of correctness of simulation, and for speeding-up the code. The advantage is that in a single file all the results relative to magnetic measurements of all LHC magnets are available, in a rather user-friendly format. The drawbacks are that the size of the file WISE.XLS grows and that it has resulted in many sheets inside WISE. This might be corrected in the future by using an informatics interface to FiDeL [3]. The last time measurements have been updated is shown in the *Summary* sheet (Fig. 5). This can help to ascertain if WISE needs update before simulation. Data typically evolves slowly. For most purposes a monthly update should be sufficient.

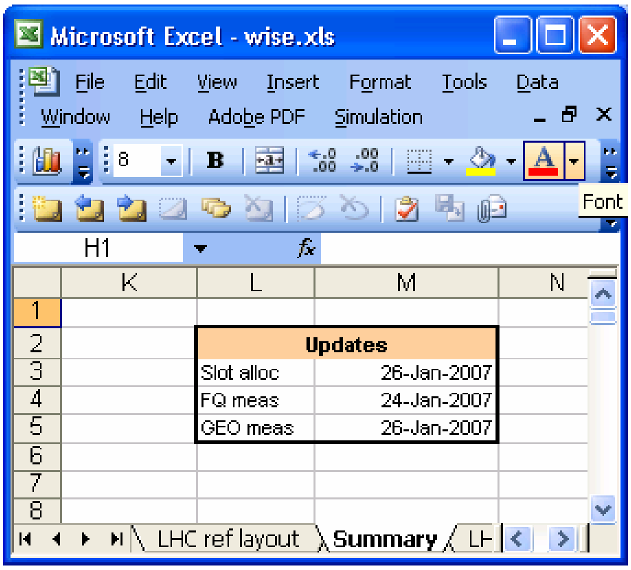


Fig. 5. The Updates table in the *Summary* sheet

### *2.3.1 Updating field quality worksheets*

The field quality measurements are updated by using the menu option in Fig. 2: *Load FQ measurements*. This operation takes some time to complete, typically 15-30 minutes depending upon several conditions impossible to predict (network load, database load, speed of local PC). The naming convention for the field quality sheet is as follows, where *MagnetType* should be replaced by the actual magnet type, like *MB:*

- *MagnetType CM FQ* is used for room temperature measurements of the cold mass.
- *MagnetType INJ FQ* is used for “cold” measurements around injection energy.
- *MagnetType COL FQ* is used for “cold” measurements around collision energy.

The data format is almost the same for all the sheets. Fig. 6 shows the beginning of the sheet *MB COL FQ*. The top rows of the sheet contain statistics that is automatically updated. There is one record per magnet aperture, roughly divided into the following logical chunks (left to right):

- identification (magnet or cold mass, aperture)
- measurement current (excitation, in A)
- magnetic length, main field and integrated main field (normalised with current, in T/A and Tm/A respectively for the dipoles)
- other multipoles expressed in units of main field

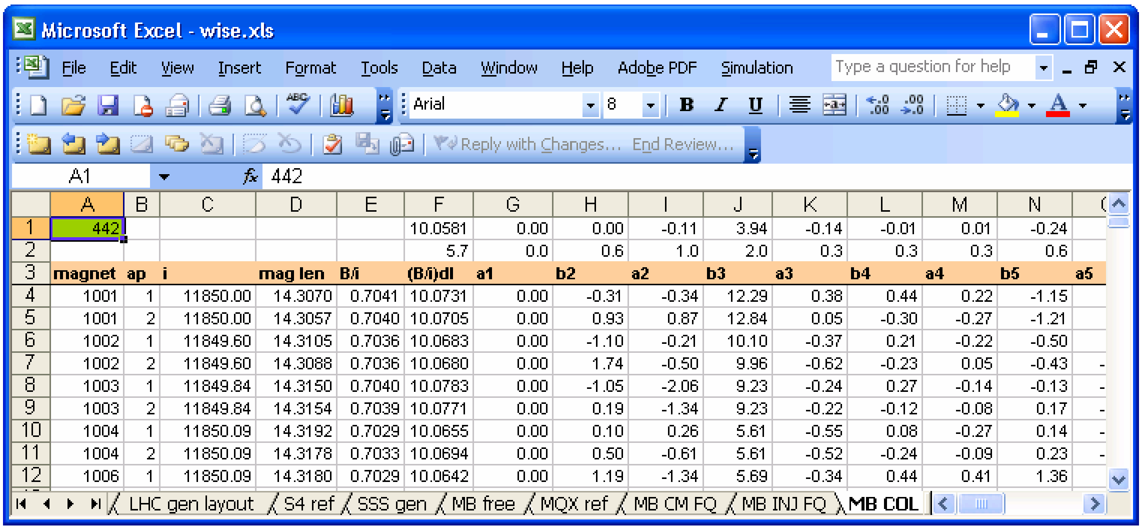

| | A | B | C | D | E | F | G | H | I | J | K | L | M | N |
|---|---|---|---|---|---|---|---|---|---|---|---|---|---|---|
| 1 | 442 | | | | | 10.0581 | 0.00 | 0.00 | -0.11 | 3.94 | -0.14 | -0.01 | 0.01 | -0.24 |
| 2 | | | | | | 5.7 | 0.0 | 0.6 | 1.0 | 2.0 | 0.3 | 0.3 | 0.3 | 0.6 |
| 3 | magnet | ap | i | mag len | B/i | (B/i)dl | a1 | b2 | a2 | b3 | a3 | b4 | a4 | b5 |
| 4 | 1001 | 1 | 11850.00 | 14.3070 | 0.7041 | 10.0731 | 0.00 | -0.31 | -0.34 | 12.29 | 0.38 | 0.44 | 0.22 | -1.15 |
| 5 | 1001 | 2 | 11850.00 | 14.3057 | 0.7040 | 10.0705 | 0.00 | 0.93 | 0.87 | 12.84 | 0.05 | -0.30 | -0.27 | -1.21 |
| 6 | 1002 | 1 | 11849.60 | 14.3105 | 0.7036 | 10.0683 | 0.00 | -1.10 | -0.21 | 10.10 | -0.37 | 0.21 | -0.22 | -0.50 |
| 7 | 1002 | 2 | 11849.60 | 14.3088 | 0.7036 | 10.0680 | 0.00 | 1.74 | -0.50 | 9.96 | -0.62 | -0.23 | 0.05 | -0.43 |
| 8 | 1003 | 1 | 11849.84 | 14.3150 | 0.7040 | 10.0783 | 0.00 | -1.05 | -2.06 | 9.23 | -0.24 | 0.27 | -0.14 | -0.13 |
| 9 | 1003 | 2 | 11849.84 | 14.3154 | 0.7039 | 10.0771 | 0.00 | 0.19 | -1.34 | 9.23 | -0.22 | -0.12 | -0.08 | 0.17 |
| 10 | 1004 | 1 | 11850.09 | 14.3192 | 0.7029 | 10.0655 | 0.00 | 0.10 | 0.26 | 5.61 | -0.55 | 0.08 | -0.27 | 0.14 |
| 11 | 1004 | 2 | 11850.09 | 14.3178 | 0.7033 | 10.0694 | 0.00 | 0.50 | -0.61 | 5.61 | -0.52 | -0.24 | -0.09 | 0.23 |
| 12 | 1006 | 1 | 11850.09 | 14.3180 | 0.7029 | 10.0642 | 0.00 | 1.19 | -1.34 | 5.69 | -0.34 | 0.44 | 0.41 | 1.36 |



Fig. 6. The *MB COL FQ* sheet with field quality measurements of main dipoles

### 2.3.2 Updating geometry worksheets

The geometry measurements are updated by using the menu option in Fig. 2: *Load GEO measurements*. This operation takes typically a couple of minutes to complete. The measurements are made after "cold test", at room temperature, in WP08 (dipoles) and WP18 (quadrupoles).

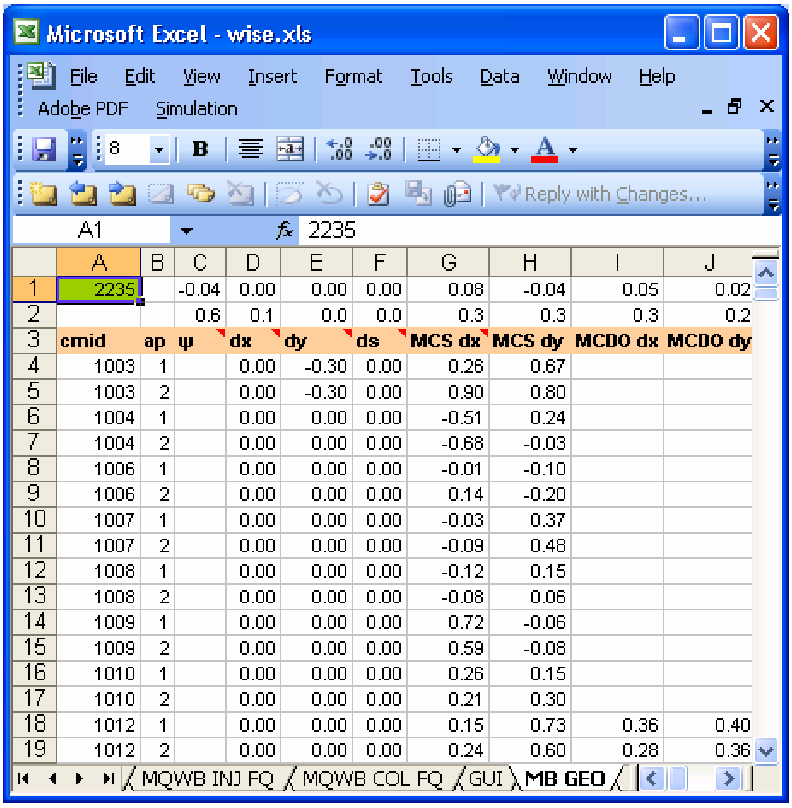

| | A | B | C | D | E | F | G | H | I | J |
|---|---|---|---|---|---|---|---|---|---|---|
| 1 | 2235 | | -0.04 | 0.00 | 0.00 | 0.00 | 0.08 | -0.04 | 0.05 | 0.02 |
| 2 | | | 0.6 | 0.1 | 0.0 | 0.0 | 0.3 | 0.3 | 0.3 | 0.2 |
| 3 | cmid | ap | ψ | dx | dy | ds | MCS dx | MCS dy | MCDO dx | MCDO dy |
| 4 | 1003 | 1 | | 0.00 | -0.30 | 0.00 | 0.26 | 0.67 | | |
| 5 | 1003 | 2 | | 0.00 | -0.30 | 0.00 | 0.90 | 0.80 | | |
| 6 | 1004 | 1 | | 0.00 | 0.00 | 0.00 | -0.51 | 0.24 | | |
| 7 | 1004 | 2 | | 0.00 | 0.00 | 0.00 | -0.68 | -0.03 | | |
| 8 | 1006 | 1 | | 0.00 | 0.00 | 0.00 | -0.01 | -0.10 | | |
| 9 | 1006 | 2 | | 0.00 | 0.00 | 0.00 | 0.14 | -0.20 | | |
| 10 | 1007 | 1 | | 0.00 | 0.00 | 0.00 | -0.03 | 0.37 | | |
| 11 | 1007 | 2 | | 0.00 | 0.00 | 0.00 | -0.09 | 0.48 | | |
| 12 | 1008 | 1 | | 0.00 | 0.00 | 0.00 | -0.12 | 0.15 | | |
| 13 | 1008 | 2 | | 0.00 | 0.00 | 0.00 | -0.08 | 0.06 | | |
| 14 | 1009 | 1 | | 0.00 | 0.00 | 0.00 | 0.72 | -0.06 | | |
| 15 | 1009 | 2 | | 0.00 | 0.00 | 0.00 | 0.59 | -0.08 | | |
| 16 | 1010 | 1 | | 0.00 | 0.00 | 0.00 | 0.26 | 0.15 | | |
| 17 | 1010 | 2 | | 0.00 | 0.00 | 0.00 | 0.21 | 0.30 | | |
| 18 | 1012 | 1 | | 0.00 | 0.00 | 0.00 | 0.15 | 0.73 | 0.36 | 0.40 |
| 19 | 1012 | 2 | | 0.00 | 0.00 | 0.00 | 0.24 | 0.60 | 0.28 | 0.36 |



Fig. 7. The sheet *MB GEO* with geometry measurements

The following sheets are used:

- *MB GEO* for magnets in MB cryostats.
- *MQ GEO* for magnets in MQ cryostats.

- *S4 GEO* for quadrupoles in special short straight sections.

- *X GEO* for single aperture magnets around the IPs (inner triplets Q1-3 and separation dipoles D1)

The start of the *MB GEO* sheet is shown in Fig. 7. The data format is almost the same for all the sheets. The top rows of the sheet contain statistics that is automatically updated. There is one record per magnet aperture, containing (left to right):

- identification (magnet or cold mass, aperture)

- field angle

- position of cryostat (i.e., installation shifts)

- position of individual magnets relative to the cold mass mean plane.

#### *2.3.3 Updating slot allocations*

The sheet *LHC ref layout* contains the layout of the LHC machine as well as the actual slot allocation from, both official and pre-allocated by project engineers. This information is then copied into the sheet *LHC gen layout* and empty slots are drawn as explained in section 5. *LHC gen layout* is the actual sheet used during simulation. The slot allocation is updated manually using the menu option *Update slot allocation…* in Fig. 2.

The steady progress of completing the installation of LHC led to the idea that a complete slot allocation should be done more infrequently and manually. The menu option *Generate LHC layout with all slots allocated* (Fig. 2) is how to manually produce the sheet *LHC gen layout*. This action is used in combination with option *Use current LHC slot layout* (Fig. 4). Once LHC is completed the slot allocation code is no longer needed, except for *what if* scenarios for spare magnets.

The beginning of the *LHC ref layout* sheet is shown in Fig. 8. One record is used for each magnet. Each column comes from a separate source of information:

- *SSSCoord* for main quadrupole pre-allocated by the SSS coordinator.

- *S4Coord* for insertion quadrupoles pre-allocated by the S4 coordinator.

- *MTF* and *MTF Res* for official slot allocations, either installed or reserved (i.e. allocated by MEB).

- *Override* for your own allocations taking precedence over the others sources.

The result of all these sources is merged into the *cryostat* column. This is the only column used during the simulation. If the sources give conflicting information, the cryostat column is coloured red, but be aware that overrides are blindly applied and leave no red!

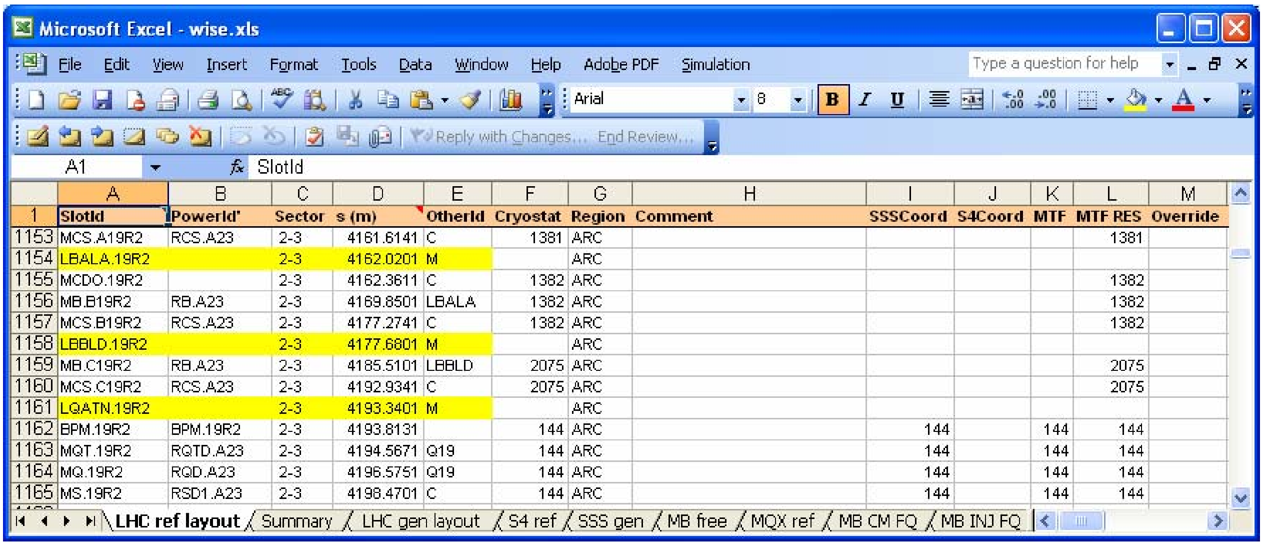

| 1 | SlotId | PowerId' | Sector | s (m) | OtherId | Cryostat | Region | Comment | SSSCoord | S4Coord | MTF | MTF RES | Override |
|---|---|---|---|---|---|---|---|---|---|---|---|---|---|
| 1153 | MCS.A19R2 | RCS.A23 | 2-3 | 4161.6141 | C | 1381 | ARC | | | | | 1381 | |
| 1154 | LBALA.19R2 | | 2-3 | 4162.0201 | M | | ARC | | | | | | |
| 1155 | MCDO.19R2 | | 2-3 | 4162.3611 | C | 1382 | ARC | | | | | 1382 | |
| 1156 | MB.B19R2 | RB.A23 | 2-3 | 4169.8501 | LBALA | 1382 | ARC | | | | | 1382 | |
| 1157 | MCS.B19R2 | RCS.A23 | 2-3 | 4177.2741 | C | 1382 | ARC | | | | | 1382 | |
| 1158 | LBBLD.19R2 | | 2-3 | 4177.6801 | M | | ARC | | | | | | |
| 1159 | MB.C19R2 | RB.A23 | 2-3 | 4185.5101 | LBBLD | 2075 | ARC | | | | | 2075 | |
| 1160 | MCS.C19R2 | RCS.A23 | 2-3 | 4192.9341 | C | 2075 | ARC | | | | | 2075 | |
| 1161 | LQATN.19R2 | | 2-3 | 4193.3401 | M | | ARC | | | | | | |
| 1162 | BPM.19R2 | BPM.19R2 | 2-3 | 4193.8131 | | 144 | ARC | | 144 | | 144 | 144 | |
| 1163 | MQT.19R2 | RQTD.A23 | 2-3 | 4194.5671 | Q19 | 144 | ARC | | 144 | | 144 | 144 | |
| 1164 | MQ.19R2 | RQD.A23 | 2-3 | 4196.5751 | Q19 | 144 | ARC | | 144 | | 144 | 144 | |
| 1165 | MS.19R2 | RSD1.A23 | 2-3 | 4198.4701 | C | 144 | ARC | | 144 | | 144 | 144 | |

Fig. 8. The sheet *LHC Ref Layout* with known slot allocations

## 2.4 The output files from WISE

We assume that the *Simulation Name* we gave in Fig. 3 is *mb.*

- The WISE output files for the magnetic field simulation are

  *mb-emfq-0001.tfs*
  *mb-emfq-0002.tfs*
  *mb-emfq-0003.tfs*
  …

  The files contain magnetic field errors expressed as normal and skew multipoles. It is a sparse matrix implemented as .TFS tables with the 2x15 first multipoles, both beams. WISE provides template MAD-X scripts to process these tables. The progressive number identifies each instance of the simulation.

- The WISE output files for the geometry simulation are

  *mb-egeose-0001-b1.tfs*
  *mb-egeose-0001-b2.tfs*
  *mb-egeose-0002-b1.tfs*
  *mb-egeose-0002-b2.tfs*
  …

  These files contain the geometric imperfections expressed as displacements relative to the unperturbed machine. Also in this case, the progressive number identifies each instance of the machine.

- Optional MAD-X scripts

  The template scripts generated to ease running of MAD-X with the different instances of the machine are

  *mb-b1*
  *mb-b2*

*mb-wrapper-b1*
*mb-wrapper-b2*

*mb-b1.madx*
*mb-b2.madx*

*mb-cmfq-0001.madx*
...
*mb-cmfq-0030.madx*

- The files *mb-b1* and *mb-b2* are the script (one per beam) to be called for executing the MAD simulation (one or more iterations). They call the wrapper *mb-wrapper-b1* once for each iteration. *b1* means beam 1. This wrapper in turn calls the MAD-X executable with the script *mb-b1.madx*. That is, the same script is used for all the iterations. *mb-b1.madx* is a skeleton script made by WISE. It needs adaptation to specific needs. This could for example be if you want to implement some correction of optical errors, needing some specific output from WISE or doing particle tracking. The script is generated as a function of what options you have selected in the WISE so often you do not need to touch the script.

- The script *mb-b1.madx* uses fixed file names. That is, names of input and output file names are the same for all iterations. Therefore, each simulation must be run one by one (serialised). The simulation of both beams can be run in parallel (no need for serialization). In addition, simulation with different names can be run in parallel without risk of file names clashes.

- The files *mb-cmfq-nnnn.madx* are used for the optional powering of correctors. Currently they are only used for the MB spool pieces. The spool pieces must be powered since analytic calculations show they give an important contribution to field errors due to misalignment. The nominal LHC optics files do not assign strength to corrector magnets. The powering of other corrector magnets depends upon correction strategy used in the machine and is outside the scope of the WISE implementation. It would typically be an iterative feedback process trying to optimise one or more optics variables in the machine. WISE only gives the initial error estimates and powering of spool pieces.

During simulation the output results are first written to intermediate worksheets. Each sheet keeps the last iteration before being subsequently overwritten. They exist for the sake of making verification of simulation easier inside Excel, as well as they contain information details not present in the MAD-X .TFS tables. The details will be revealed in section 3 to 5. The sheets are:

- MAD FQ errors for error sources powering and magnetic field

- MAD GEO errors for geometry and tunnel misalignment

### 2.5 Log of known issues

At the bottom of the *Summary* sheet in WISE.XLS you find a log of the progress of the software implementation as well as pending issues.

### 2.6 Using the WISE output files with MAD-X scripts of your own choice

To demonstrate a more versatile use of the WISE output files we show in the following a small MAD-X script that uses the output files described in 2.4 for the 1st instance. Lines starting with exclamation mark ( ! ) are used for commenting the script. The script is limited to beam 1 at injection using LHC thick lens model. The WISE specific code is in bold. The extension of the script to process several instances of imperfections is left as an exercise for the reader.

```
! link to LHC optics parent directory
system,    "ln -fns /afs/cern.ch/eng/lhc/optics do";
! link to LHC MAD-X support scripts
system,    "ln -fns /afs/cern.ch/eng/lhc/optics/V6.500/measured_errors dm";

! LHC optics layout as function of optics lens model
option,    -info, -warn, verify, -echo;
call,      file="do/V6.500/V6.5.seq";

! LHC optics strength as function of lens model, cycle and beam
call,      file="do/V6.500/V6.5.inj.str";
beam,      sequence=lhcb1,particle=proton,energy=450,kbunch=2808,npart=1.15E11;
use,       sequence=lhcb1; mylhcbeam=1;

! Scripts tailored for measured errors in LHC
call,      file="dm/Msubroutines.madx";
call,      file="dm/Ealign_Subroutines.madx";

! Activate multipoles except b1, a1 when processing field quality table
exec, ON_SYST;
ON_B1S = 0; ON_A1S = 0;

eoption,add=true;

! WISE geometry
readtable, file="~/mb-egeo-0001-b1.tfs";
exec, Ealign_All;

! Rotations of magnets into tunnel reference frame
readtable, file="dm/rotations.tab";

! WISE magnetic field quality (both beams and all magnet types in same table)
readtable, file="~/mb-emfqcs-0001.tfs";
call,      file="dm/Efcomp_MB.madx";

! WISE corrector strength for spool pieces
call,      file="~/mb-cmfq-0001.madx";

! End of WISE assigned imperfections and your code continues here
```

## 3. DETAILS ON MAGNETIC FIELD QUALITY

The simulation of magnetic field quality is driven by two sources of errors:

- Best estimate based on measurements $E^t$, with the associated uncertainties $\Delta$ (both due to the measurement system $\Delta E^m$ and due to powering history of the magnet $\Delta E^h$).
- Variation of the main field due to power supply uncertainties $\Delta E^p$

Let $E$ be either the transfer function or a multipole of a magnet labelled by $j$. We then have

$$E_j = E_j^t + \Delta E_j^m + \Delta E_j^h + \Delta E_j^p \tag{1}$$

The field quality errors are expressed in *units* of the main field, where by definition: 1 unit $=10^{-4}$ · The main field itself is also expressed in units, with respect to the nominal values stored in the Table *Magnetic field quality* (see Fig. 9).

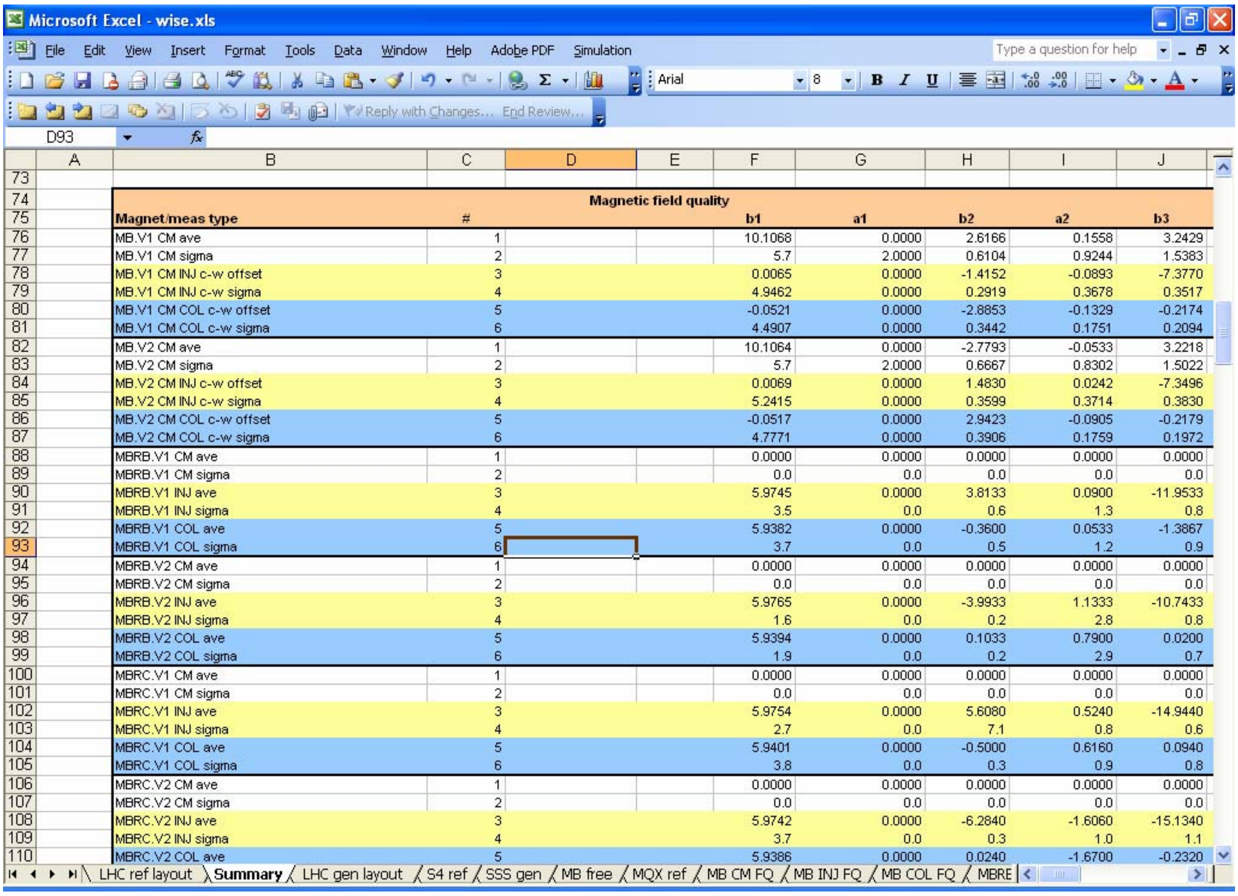

| Magnet/meas type | # | b1 | a1 | b2 | a2 | b3 |
|---|---|---|---|---|---|---|
| MB.V1 CM ave | 1 | 10.1068 | 0.0000 | 2.6166 | 0.1558 | 3.2429 |
| MB.V1 CM sigma | 2 | 5.7 | 2.0000 | 0.6104 | 0.9244 | 1.5383 |
| MB.V1 CM INJ c-w offset | 3 | 0.0065 | 0.0000 | -1.4152 | -0.0893 | -7.3770 |
| MB.V1 CM INJ c-w sigma | 4 | 4.9462 | 0.0000 | 0.2919 | 0.3678 | 0.3517 |
| MB.V1 CM COL c-w offset | 5 | -0.0521 | 0.0000 | -2.8853 | -0.1329 | -0.2174 |
| MB.V1 CM COL c-w sigma | 6 | 4.4907 | 0.0000 | 0.3442 | 0.1751 | 0.2094 |
| MB.V2 CM ave | 1 | 10.1064 | 0.0000 | -2.7793 | -0.0533 | 3.2218 |
| MB.V2 CM sigma | 2 | 5.7 | 2.0000 | 0.6667 | 0.8302 | 1.5022 |
| MB.V2 CM INJ c-w offset | 3 | 0.0069 | 0.0000 | 1.4830 | 0.0242 | -7.3496 |
| MB.V2 CM INJ c-w sigma | 4 | 5.2415 | 0.0000 | 0.3599 | 0.3714 | 0.3830 |
| MB.V2 CM COL c-w offset | 5 | -0.0517 | 0.0000 | 2.9423 | -0.0905 | -0.2179 |
| MB.V2 CM COL c-w sigma | 6 | 4.7771 | 0.0000 | 0.3906 | 0.1759 | 0.1972 |
| MBRB.V1 CM ave | 1 | 0.0000 | 0.0000 | 0.0000 | 0.0000 | 0.0000 |
| MBRB.V1 CM sigma | 2 | 0.0 | 0.0 | 0.0 | 0.0 | 0.0 |
| MBRB.V1 INJ ave | 3 | 5.9745 | 0.0000 | 3.8133 | 0.0900 | -11.9533 |
| MBRB.V1 INJ sigma | 4 | 3.5 | 0.0 | 0.6 | 1.3 | 0.8 |
| MBRB.V1 COL ave | 5 | 5.9382 | 0.0000 | -0.3600 | 0.0533 | -1.3867 |
| MBRB.V1 COL sigma | 6 | 3.7 | 0.0 | 0.5 | 1.2 | 0.9 |
| MBRB.V2 CM ave | 1 | 0.0000 | 0.0000 | 0.0000 | 0.0000 | 0.0000 |
| MBRB.V2 CM sigma | 2 | 0.0 | 0.0 | 0.0 | 0.0 | 0.0 |
| MBRB.V2 INJ ave | 3 | 5.9765 | 0.0000 | -3.9933 | 1.1333 | -10.7433 |
| MBRB.V2 INJ sigma | 4 | 1.6 | 0.0 | 0.2 | 2.8 | 0.8 |
| MBRB.V2 COL ave | 5 | 5.9394 | 0.0000 | 0.1033 | 0.7900 | 0.0200 |
| MBRB.V2 COL sigma | 6 | 1.9 | 0.0 | 0.2 | 2.9 | 0.7 |
| MBRC.V1 CM ave | 1 | 0.0000 | 0.0000 | 0.0000 | 0.0000 | 0.0000 |
| MBRC.V1 CM sigma | 2 | 0.0 | 0.0 | 0.0 | 0.0 | 0.0 |
| MBRC.V1 INJ ave | 3 | 5.9754 | 0.0000 | 5.6080 | 0.5240 | -14.9440 |
| MBRC.V1 INJ sigma | 4 | 2.7 | 0.0 | 7.1 | 0.8 | 0.6 |
| MBRC.V1 COL ave | 5 | 5.9401 | 0.0000 | -0.5000 | 0.6160 | 0.0940 |
| MBRC.V1 COL sigma | 6 | 3.8 | 0.0 | 0.3 | 0.9 | 0.8 |
| MBRC.V2 CM ave | 1 | 0.0000 | 0.0000 | 0.0000 | 0.0000 | 0.0000 |
| MBRC.V2 CM sigma | 2 | 0.0 | 0.0 | 0.0 | 0.0 | 0.0 |
| MBRC.V2 INJ ave | 3 | 5.9742 | 0.0000 | -6.2840 | -1.6060 | -15.1340 |
| MBRC.V2 INJ sigma | 4 | 3.7 | 0.0 | 0.3 | 1.0 | 1.1 |
| MBRC.V2 COL ave | 5 | 5.9386 | 0.0000 | 0.0240 | -1.6700 | -0.2320 |

Fig. 9. The *Magnetic field quality* statistics table in the *Summary* sheet

### 3.1 Magnetic field

The static magnetic field imperfections are mainly due to the coil geometry. These errors are the most important ones and are usually measured for each magnet and aperture. They must be estimated based upon statistics for magnets not yet built or when data are missing. Only a fraction of the LHC magnets for the lattice has been measured in operational "cold" conditions, as part of production sampling. In these conditions one can measure the effect of persistent currents, and other effects as iron saturation, deformation due to cool-down and Lorentz forces. Room temperature measurements plus a warm-to-cold correlation is used to estimate the operating condition when cold measurements are not available. Such correlations have an uncertainty which is estimated from measurements.

Field errors also have time-dependent, dynamic effects during normal operation, mainly decay and snap-back, and induced eddy-currents during ramp-up. The WISE simulation tool can only deal with static errors (time invariant) for the two major machine states: *injection* and around *collision* energy. This is in harmony with the normal MAD-X usage. The FiDel project [3] aims at providing a dynamic field model for each magnet type. WISE will change in the future to retrieve such dynamic data from FiDeL.

We will now describe the most essential calculation of the magnetic field errors, both for main field and multipoles. The "true" value $E^t$ (see Eq. 1) is computed according to availability of measurement data. The following scenario explains all the variants.

*3.1.1 Magnet measured at "cold"*

Eq. (2) is used for a magnet measured at "cold" working conditions (highest priority)

$$E_j^t = E_j^c \qquad (2)$$

It just expresses the fact that we are using the "cold" measurement "as is", since it is the best available information.

*3.1.2 Measured at "warm"*

$$E_j^t = E_j^w + E_k^{c-w} + \Delta E_j^{c-w} \qquad (3)$$

Eq. (3) is used for a magnet measured at "warm" room temperature. The warm-to-cold correlation for the magnet type is added with two terms: systematic effect and an individual drawn Gaussian uncertainty truncated to 3σ. Both the systematic and the standard deviation depend on the magnet type *k*, and are read from the table described in section 3.1.4, which is evaluated "off-line" from measurements.

*3.1.3 Magnet not yet produced (no measurement)*

Eqs. (4) and (5) are used for a magnet where no measurement data is available. In most cases, the magnet is generated at warm by taking the systematic effect and draw a Gaussian value truncated to 3σ for the individual production spread

$$E_j^w = \overline{E}^w + \Delta E_j^w \qquad (4)$$

The resulting error is then substituted in Eq. (3). For some magnet types we have no values at warm (this happens when they are all measured at cold) – in this case they are generated directly at cold

$$E_j^c = \overline{E}^c + \Delta E_j^c \qquad (5)$$

The resulting error is then substituted into equation 2.

*3.1.4 Field quality statistics table*

Eqs. (3,4,5) require the knowledge of the distribution of errors for various quantities. This information is calculated in the table used shown in Fig. 9, containing average and standard deviations of room temperature measurements, and of the offsets between warm measurements and operational conditions (both injection and high field). This table is maintained manually. Therefore some values in the table might differ from the results of the raw statistics in the measurement sheets shown in Fig. 6. Statistics is separated for aperture 1 and 2 to correctly deal with even normal multipoles for the main dipoles.

The Table of Fig. 9 is a large for several reasons. It contains all major magnet types for LHC. Each entry contains of 6 rows and describes one class of magnets. The table has column space for all 30 multipoles present in LHC magnetic measurements. The last 4 or 5 is probably overkill but comes for "free" in the implementation. For the averages, the measurement units in the table are the integrated strength for the main field, and units of main field for all other multipoles. Example: ∫(B/i)dl for dipoles and ∫(G/i)dl for quadrupoles. All standard deviations are expressed in units.

The two first rows (1+2) of a magnet class are dedicated to room temperature data (average, sigma). Rows 3+ 4 are for injection ("*INJ*") and 5+6 for collision ("*COL*"). The magnet class using "warm" data and "warm-to-cold" correlations has the text "c-w offset" and "c-w sigma" in rows 3-6. They relate to the equations 3 and 4. Example: *MB.V1*. The classes using "cold" data directly have the text "ave" and "sigma" in rows 3-6 and relate to equation 5. In this case, the "warm" rows 1+2 are not used for these (0s). Example: *MBRB.V1.*

*3.1.5 Transfer function tuning using power supply*

WISE knows which magnets and apertures share the same power supply. By default, the average integrated transfer function error of the set of magnets connected to the same power supply is set to zero. This is equivalent to assume that the power supply is adjusted to compensate imperfections of the average transfer function. For instance, the average of the transfer function error taken over the dipoles belonging to the same sector is zero. This option can be disabled in the *Run Simulation/Options* menu (see section 2.2): *Do not adjust power.*

*3.1.6 Hysteresis magnetisation effects*

In section 3.1 we stated that WISE can only deal with injection and high field errors. However, both MQM and MQY are powered at injection and at high field with individual currents that are not related to nominal values used for magnet acceptance. To solve this problem, the option of downloading the measurements for several values of the field current has not been followed. Instead, we used the FiDeL equation [6] giving the dependence of the allowed multipoles $b_6$ and $b_{10}$ on the current

$$b_n(i) = \mu_n \left( \frac{i_{inj}}{i} \right)^{2-p_n} \left( \frac{i_c - i}{i_c - i_{inj}} \right)^{q_n} \tag{6}$$

where $i_{inj}$ is the current at injection, $i_c$ is the so called "critical" current (the transition point from super-conducting to resistive state), and the fitting parameters are in the *Summary sheet* (see Fig. 10). This equation is used to reconstruct the $b_6$ and $b_{10}$ error values when the operational current is different from the measured one. This option is applied only to MQY and MQM.

The actual value of the field strength is given by a MAD input file. An extra Excel utility was made to dump the optics strength of the various official LHC optics files, see the 2 last menu options in Fig. 2. The subfolder *Studies* of the WISE simulation contains the file *lhc-strength.xls* for processing the dump from MAD-X. This produces the sheet *Q K1L* shown in Fig. 11: the column *NAME* contains the optical slot id as defined by MAD-X. The *L* column is for the nominal magnetic length and is supposed to be constant for each magnet type. Then there is one column for each optics scenario containing the normalised strength. Example *V6.5.inj B1* means beam 1 at injection using LHC layout version 6.5. The current corresponding to a given gradient K1L is computed according to

$$i = 10^3 B_{arc} \rho_0 \frac{K_{1L}}{lG} \tag{7}$$

Where $B_{arc}$ and $\rho_0$ are the bending strength and bending reference radius stored in the *Summary* sheet (Fig. 12), $l$ is the magnetic length, $K_{1L}$.is the integrated, normalised gradient of the quadrupole (Fig. 13), and $G$ is the nominal gradient.

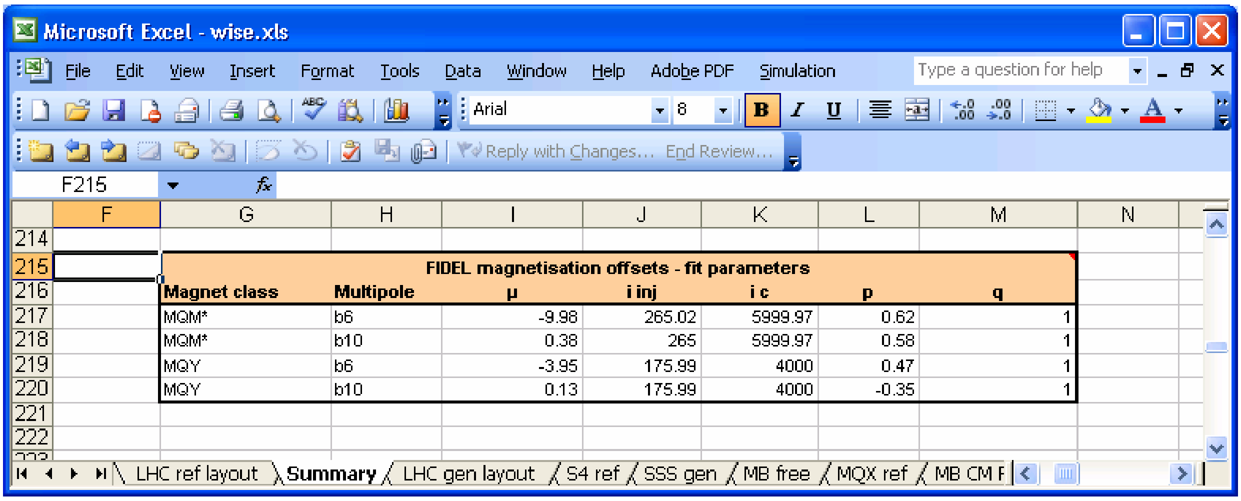


| FIDEL magnetisation offsets - fit parameters | | | | | | |
|---|---|---|---|---|---|---|
| Magnet class | Multipole | μ | i inj | i c | p | q |
| MQM* | b6 | -9.98 | 265.02 | 5999.97 | 0.62 | 1 |
| MQM* | b10 | 0.38 | 265 | 5999.97 | 0.58 | 1 |
| MQY | b6 | -3.95 | 175.99 | 4000 | 0.47 | 1 |
| MQY | b10 | 0.13 | 175.99 | 4000 | -0.35 | 1 |

Fig. 10. The FiDeL fitting parameters table in the *Summary* sheet

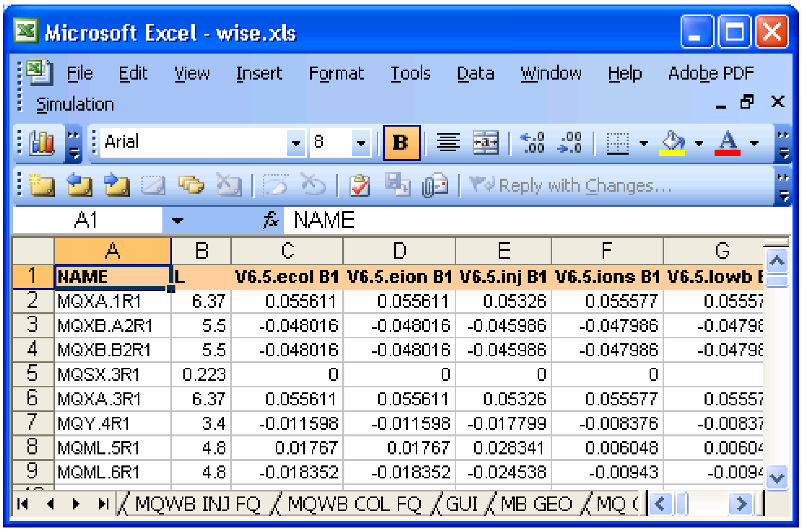


| NAME | L | V6.5.ecol B1 | V6.5.eion B1 | V6.5.inj B1 | V6.5.ions B1 | V6.5.lowb B |
|---|---|---|---|---|---|---|
| MQXA.1R1 | 6.37 | 0.055611 | 0.055611 | 0.05326 | 0.055577 | 0.05557 |
| MQXB.A2R1 | 5.5 | -0.048016 | -0.048016 | -0.045986 | -0.047986 | -0.04798 |
| MQXB.B2R1 | 5.5 | -0.048016 | -0.048016 | -0.045986 | -0.047986 | -0.04798 |
| MQSX.3R1 | 0.223 | 0 | 0 | 0 | 0 | |
| MQXA.3R1 | 6.37 | 0.055611 | 0.055611 | 0.05326 | 0.055577 | 0.05557 |
| MQY.4R1 | 3.4 | -0.011598 | -0.011598 | -0.017799 | -0.008376 | -0.00837 |
| MQML.5R1 | 4.8 | 0.01767 | 0.01767 | 0.028341 | 0.006048 | 0.0060 |
| MQML.6R1 | 4.8 | -0.018352 | -0.018352 | -0.024538 | -0.00943 | -0.0094 |

Fig. 11. The *Q K1L* sheet

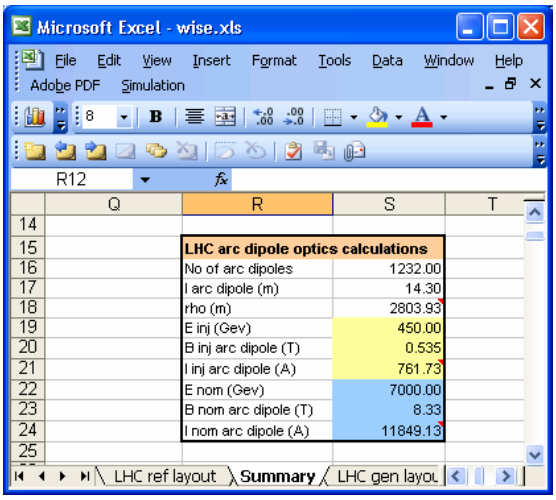


| LHC arc dipole optics calculations | |
|---|---|
| No of arc dipoles | 1232.00 |
| l arc dipole (m) | 14.30 |
| rho (m) | 2803.93 |
| E inj (Gev) | 450.00 |
| B inj arc dipole (T) | 0.535 |
| I inj arc dipole (A) | 761.73 |
| E nom (Gev) | 7000.00 |
| B nom arc dipole (T) | 8.33 |
| I nom arc dipole (A) | 11849.13 |

Fig. 12. The *LHC arc optics parameters* table in the *Summary* sheet

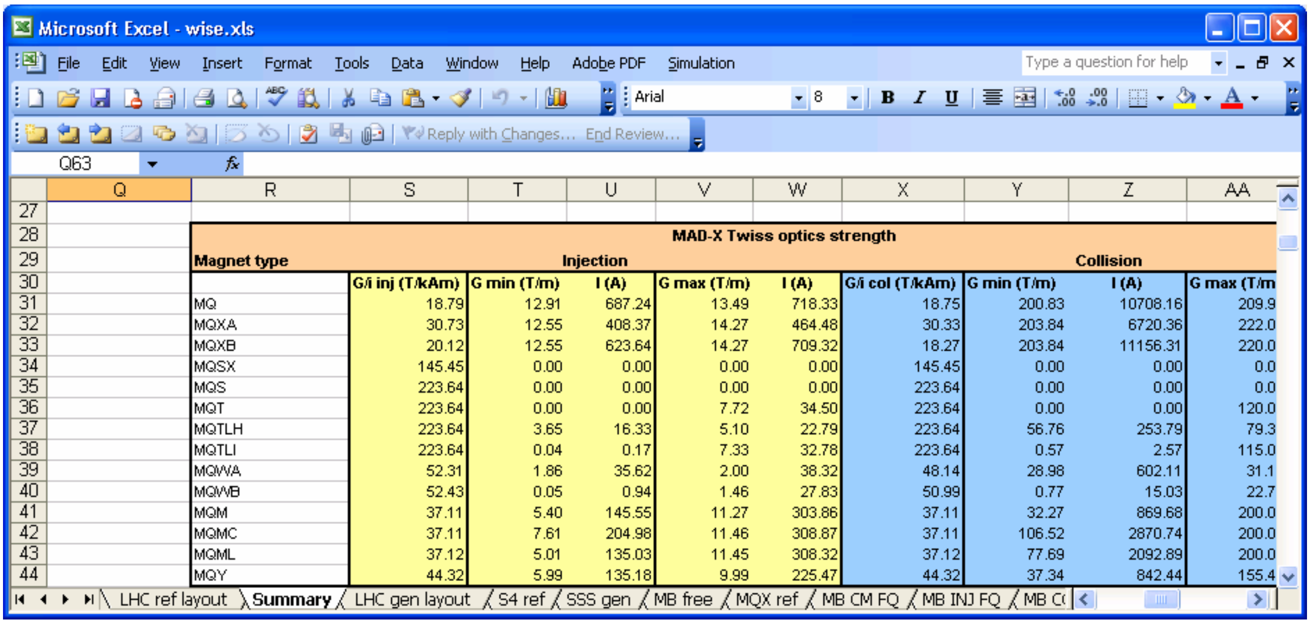

| MAD-X Twiss optics strength | | | | | | | | | |
|---|---|---|---|---|---|---|---|---|---|
| Magnet type | Injection | | | | | Collision | | | |
| | G/i inj (T/kAm) | G min (T/m) | I (A) | G max (T/m) | I (A) | G/i col (T/kAm) | G min (T/m) | I (A) | G max (T/m |
| MQ | 18.79 | 12.91 | 687.24 | 13.49 | 718.33 | 18.75 | 200.83 | 10708.16 | 209.9 |
| MQXA | 30.73 | 12.55 | 408.37 | 14.27 | 464.48 | 30.33 | 203.84 | 6720.36 | 222.0 |
| MQXB | 20.12 | 12.55 | 623.64 | 14.27 | 709.32 | 18.27 | 203.84 | 11156.31 | 220.0 |
| MQSX | 145.45 | 0.00 | 0.00 | 0.00 | 0.00 | 145.45 | 0.00 | 0.00 | 0.0 |
| MQS | 223.64 | 0.00 | 0.00 | 0.00 | 0.00 | 223.64 | 0.00 | 0.00 | 0.0 |
| MQT | 223.64 | 0.00 | 0.00 | 7.72 | 34.50 | 223.64 | 0.00 | 0.00 | 120.0 |
| MQTLH | 223.64 | 3.65 | 16.33 | 5.10 | 22.79 | 223.64 | 56.76 | 253.79 | 79.3 |
| MQTLI | 223.64 | 0.04 | 0.17 | 7.33 | 32.78 | 223.64 | 0.57 | 2.57 | 115.0 |
| MQWA | 52.31 | 1.86 | 35.62 | 2.00 | 38.32 | 48.14 | 28.98 | 602.11 | 31.1 |
| MQWB | 52.43 | 0.05 | 0.94 | 1.46 | 27.83 | 50.99 | 0.77 | 15.03 | 22.7 |
| MQM | 37.11 | 5.40 | 145.55 | 11.27 | 303.86 | 37.11 | 32.27 | 869.68 | 200.0 |
| MQMC | 37.11 | 7.61 | 204.98 | 11.46 | 308.87 | 37.11 | 106.52 | 2870.74 | 200.0 |
| MQML | 37.12 | 5.01 | 135.03 | 11.45 | 308.32 | 37.12 | 77.69 | 2092.89 | 200.0 |
| MQY | 44.32 | 5.99 | 135.18 | 9.99 | 225.47 | 44.32 | 37.34 | 842.44 | 155.4 |

Fig. 13. The MAD-X Twiss *optics strength* table in the *Summary* sheet

### *3.1.7 Beam screen*

The beam screen is not present when measuring the magnetic field, and is installed after "cold test", before the magnets goes into the tunnel. It is made of stainless steel and with a thin coating of copper. It therefore has an impact on field quality. WISE uses the best available estimates of the beam screen effect [7], which are stored in the *Summary* sheet. The calculation of beam screen magnetisation is by default enabled. The sheet *LHC ref layout* contains the type of beam screen used, with the big exception that the majority of magnets (arcs) use type "50A/V". The beam screen contribution is a systematic, adding to the previous estimates.

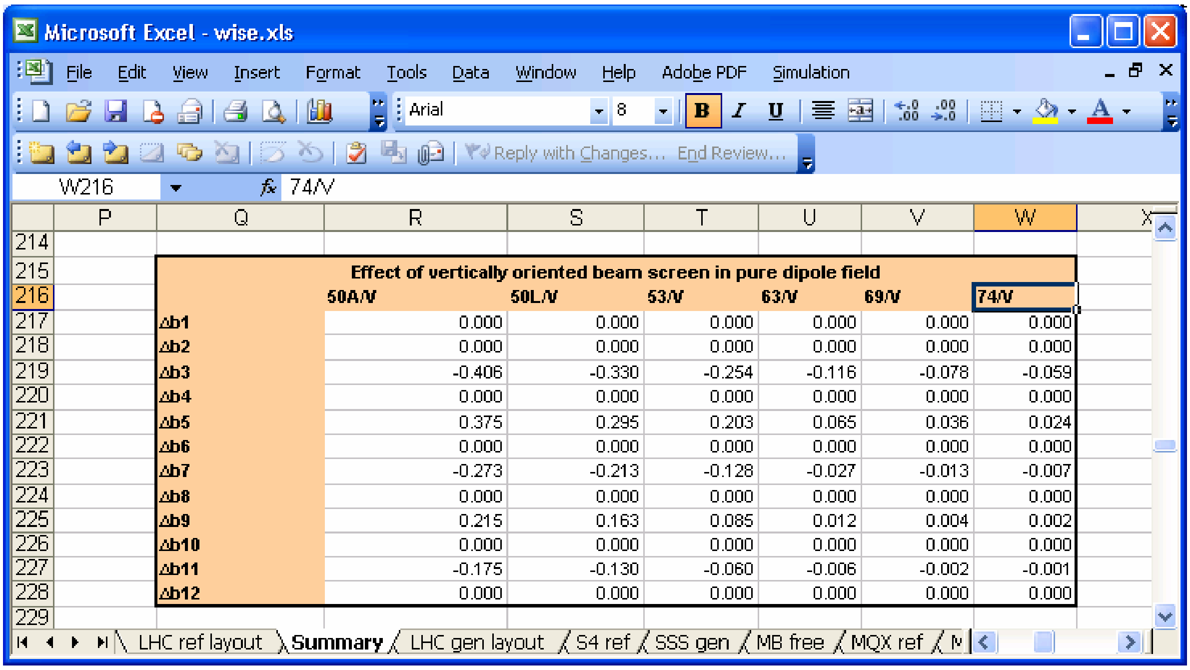

| Effect of vertically oriented beam screen in pure dipole field | | | | | | |
|---|---|---|---|---|---|---|
| | 50A/V | 50L/V | 53/V | 63/V | 69/V | 74/V |
| Δb1 | 0.000 | 0.000 | 0.000 | 0.000 | 0.000 | 0.000 |
| Δb2 | 0.000 | 0.000 | 0.000 | 0.000 | 0.000 | 0.000 |
| Δb3 | -0.406 | -0.330 | -0.254 | -0.116 | -0.078 | -0.059 |
| Δb4 | 0.000 | 0.000 | 0.000 | 0.000 | 0.000 | 0.000 |
| Δb5 | 0.375 | 0.295 | 0.203 | 0.065 | 0.036 | 0.024 |
| Δb6 | 0.000 | 0.000 | 0.000 | 0.000 | 0.000 | 0.000 |
| Δb7 | -0.273 | -0.213 | -0.128 | -0.027 | -0.013 | -0.007 |
| Δb8 | 0.000 | 0.000 | 0.000 | 0.000 | 0.000 | 0.000 |
| Δb9 | 0.215 | 0.163 | 0.085 | 0.012 | 0.004 | 0.002 |
| Δb10 | 0.000 | 0.000 | 0.000 | 0.000 | 0.000 | 0.000 |
| Δb11 | -0.175 | -0.130 | -0.060 | -0.006 | -0.002 | -0.001 |
| Δb12 | 0.000 | 0.000 | 0.000 | 0.000 | 0.000 | 0.000 |

Fig. 14. Beam screen error table for a "V"-oriented screen exposed to a dipole field

*3.1.8 Uncertainty from measurement system and magnetic history*

The $\Delta E^m$ error in equation 1 is the error due to the measurement system. It has two components:

$$\Delta E_j^m = \Delta E_j^{m,c} + \Delta E_j^{m,r} \tag{8}$$

where the first one is due to calibration, and it is assumed to be the same for all magnets of the same type, drawn from a rectangular distribution. The second contribution is related to the resolution and is neglected since the resolution of the measuring systems is always better than 1 unit.

The $\Delta E^h$ error in equation 1 is uncertainty from history in powering the magnetic field. Each magnet will have its own value drawn from a rectangular distribution.

The $\Delta E^m$ and $\Delta E^h$ errors are only applied to the main field as their influence on multipoles is very small ( ~ $10^{-8}$ to $10^{-6}$). Fig 15 shows the magnetic field uncertainty table used in the simulation.

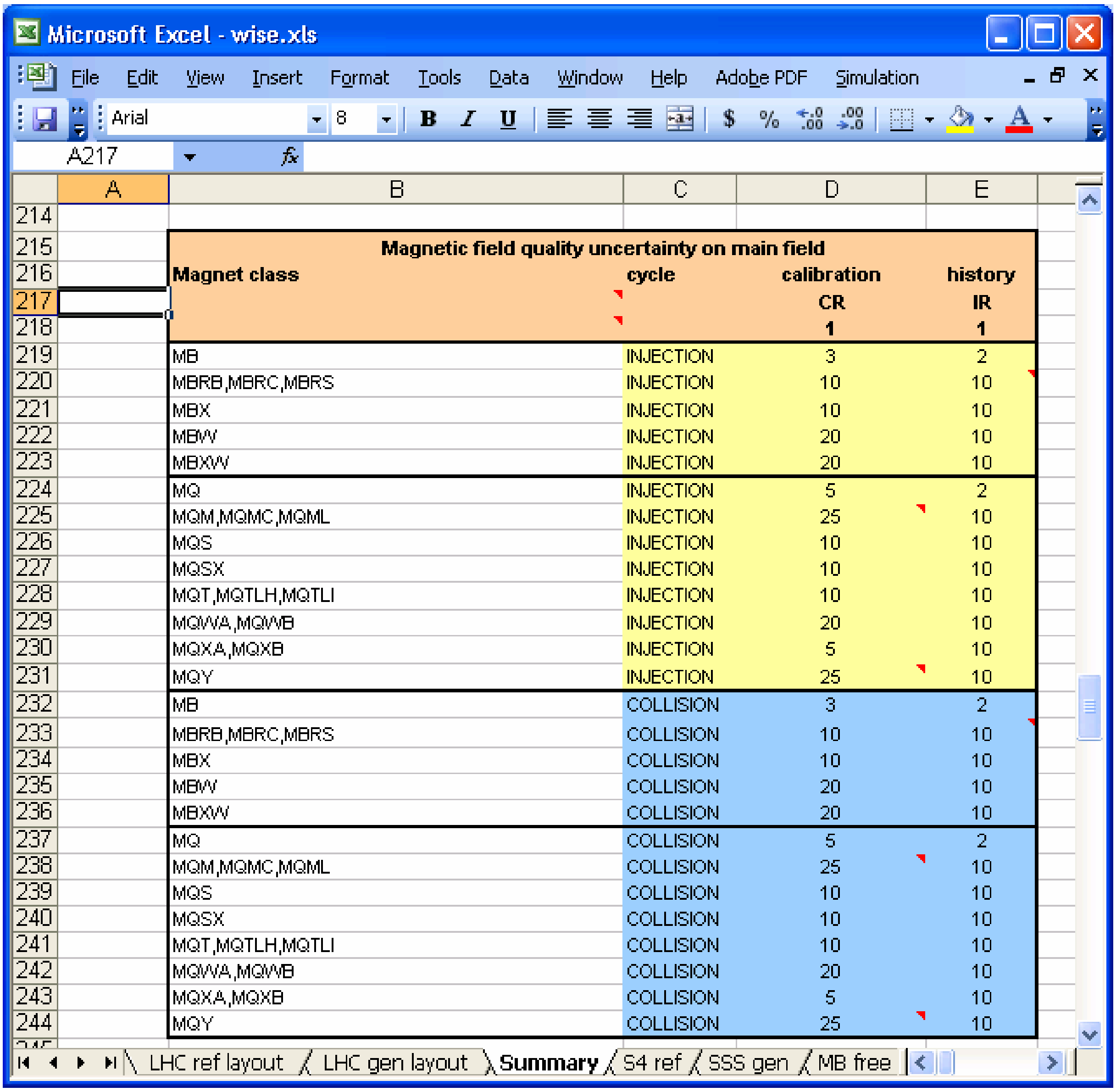


| Magnetic field quality uncertainty on main field | | | |
|---|---|---|---|
| Magnet class | cycle | calibration | history |
| | | CR | IR |
| | | 1 | 1 |
| MB | INJECTION | 3 | 2 |
| MBRB,MBRC,MBRS | INJECTION | 10 | 10 |
| MBX | INJECTION | 10 | 10 |
| MBW | INJECTION | 20 | 10 |
| MBXW | INJECTION | 20 | 10 |
| MQ | INJECTION | 5 | 2 |
| MQM,MQMC,MQML | INJECTION | 25 | 10 |
| MQS | INJECTION | 10 | 10 |
| MQSX | INJECTION | 10 | 10 |
| MQT,MQTLH,MQTLI | INJECTION | 10 | 10 |
| MQWA,MQWB | INJECTION | 20 | 10 |
| MQXA,MQXB | INJECTION | 5 | 10 |
| MQY | INJECTION | 25 | 10 |
| MB | COLLISION | 3 | 2 |
| MBRB,MBRC,MBRS | COLLISION | 10 | 10 |
| MBX | COLLISION | 10 | 10 |
| MBW | COLLISION | 20 | 10 |
| MBXW | COLLISION | 20 | 10 |
| MQ | COLLISION | 5 | 2 |
| MQM,MQMC,MQML | COLLISION | 25 | 10 |
| MQS | COLLISION | 10 | 10 |
| MQSX | COLLISION | 10 | 10 |
| MQT,MQTLH,MQTLI | COLLISION | 10 | 10 |
| MQWA,MQWB | COLLISION | 20 | 10 |
| MQXA,MQXB | COLLISION | 5 | 10 |
| MQY | COLLISION | 25 | 10 |

Fig. 15. The *Magnetic field quality uncertainty* table in the *Summary* sheet

The uncertainty table can be changed if needed as it is data driven. The "CG" and "IR" in the table header gives the error type:

- **C** as 1st letter means error applies to class: uncertainty is drawn once for each magnet type.
- **I** as 1st letter means error apply to individual magnet.
- **G** as 2nd letter means Gaussian truncated to 3σ. The value in the table is the σ of the distribution (units).
- **R** as 2nd letter means rectangular distribution and the value in the table is the half width of the distribution (units).
- **S** as 2nd letter means systematic offset from zero (units)

Under "CG" and "IR" in the table header of Fig. 15 you can see the *1* flag. Changing it to *0* disables the column below and no uncertainty is generated.

### 3.2 Uncertainty due to power supply

The $\Delta E^p$ error in Eq. (1) is the uncertainty associated to the current provided by the power supply. The estimates of the power converter uncertainties have been taken from [2]. No measurement data is involved for this error source. WISE only applies this error to the main component. The effect on other multipoles is so small that it can be ignored. These are absolute errors in current, having therefore a stronger effect at injection, approximately 16 times more than in collision. Fig 16 shows the error table used in the simulation.

The strategy for the power error simulation is as follows. A random number is drawn (rectangular distribution) for each power supply according to the magnet type. Magnets sharing the power supply will receive the same error. The common power error for magnets sharing the same power supply can be corrected. WISE knows which magnets are sharing the power supply by inspecting the sheet *LHC ref layout* which is the major table driving all simulation.

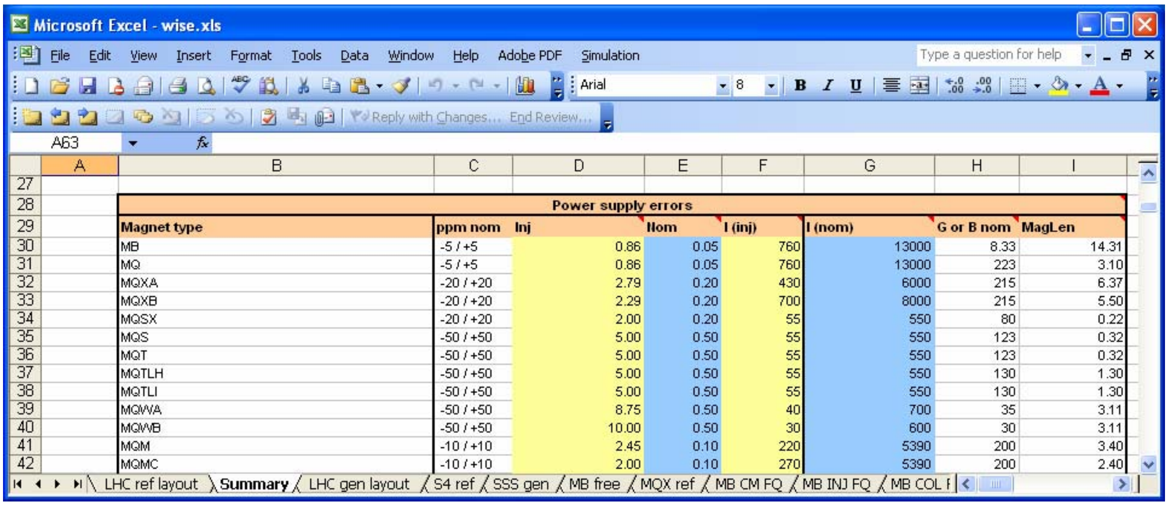

| Power supply errors | | | | | | | |
|---|---|---|---|---|---|---|---|
| Magnet type | ppm nom | Inj | Nom | I (inj) | I (nom) | G or B nom | MagLen |
| MB | -5 / +5 | 0.86 | 0.05 | 760 | 13000 | 8.33 | 14.31 |
| MQ | -5 / +5 | 0.86 | 0.05 | 760 | 13000 | 223 | 3.10 |
| MQXA | -20 / +20 | 2.79 | 0.20 | 430 | 6000 | 215 | 6.37 |
| MQXB | -20 / +20 | 2.29 | 0.20 | 700 | 8000 | 215 | 5.50 |
| MQSX | -20 / +20 | 2.00 | 0.20 | 55 | 550 | 80 | 0.22 |
| MQS | -50 / +50 | 5.00 | 0.50 | 55 | 550 | 123 | 0.32 |
| MQT | -50 / +50 | 5.00 | 0.50 | 55 | 550 | 123 | 0.32 |
| MQTLH | -50 / +50 | 5.00 | 0.50 | 55 | 550 | 130 | 1.30 |
| MQTLI | -50 / +50 | 5.00 | 0.50 | 55 | 550 | 130 | 1.30 |
| MQWA | -50 / +50 | 8.75 | 0.50 | 40 | 700 | 35 | 3.11 |
| MQWB | -50 / +50 | 10.00 | 0.50 | 30 | 600 | 30 | 3.11 |
| MQM | -10 / +10 | 2.45 | 0.10 | 220 | 5390 | 200 | 3.40 |
| MQMC | -10 / +10 | 2.00 | 0.10 | 270 | 5390 | 200 | 2.40 |

Fig. 16. The *Power supply errors* table in the *Summary* sheet

### 3.3 Powering the dipole spool pieces

A realistic powering of the spool pieces is relevant to be able to correctly simulate the feed-down effect due to the misalignment of spool pieces. For this reason, WISE provides an optional educated guess of the spool pieces currents needed to correct the field harmonics stemming from the main dipoles. This guess is based on cancellation of the integral field errors per sector.

In section 2 we mentioned the WISE output files *mb-cmfq-nnnn.madx* that are used for powering the so-called MB spool pieces. These corrector magnets exist for correcting the MB systematic errors of $b_3$, $b_4$ and $b_5$. All MBs in one sector share the same power supply. The same simulation strategy is used as for the correction of the field integral on the same power supply. The only difference being that we account beam 1 and beam 2 separately since the spool pieces have separate power supplies for the two apertures, see Fig. 17. This is the only table in the Summary sheet that is automatically updated after simulation. The values for MB spool pieces are updated, if and only if:

- The error source *Magnetic field* is selected
- At least one sector must be selected
- The magnet type MB and one of the *b3, b4, b5* multipoles are selected

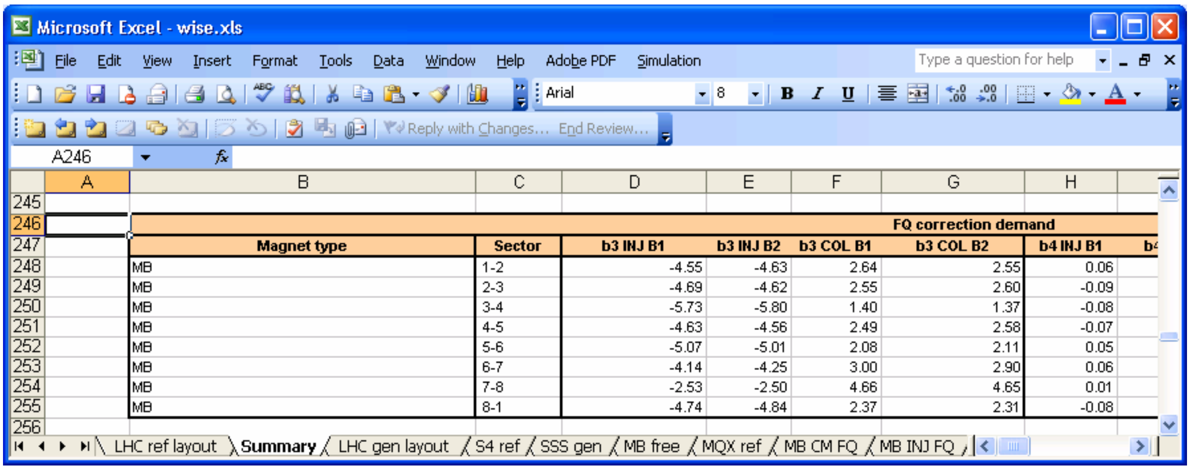

| Magnet type | Sector | b3 INJ B1 | b3 INJ B2 | b3 COL B1 | b3 COL B2 | b4 INJ B1 |
|---|---|---|---|---|---|---|
| MB | 1-2 | -4.55 | -4.63 | 2.64 | 2.55 | 0.06 |
| MB | 2-3 | -4.69 | -4.62 | 2.55 | 2.60 | -0.09 |
| MB | 3-4 | -5.73 | -5.80 | 1.40 | 1.37 | -0.08 |
| MB | 4-5 | -4.63 | -4.56 | 2.49 | 2.58 | -0.07 |
| MB | 5-6 | -5.07 | -5.01 | 2.08 | 2.11 | 0.05 |
| MB | 6-7 | -4.14 | -4.25 | 3.00 | 2.90 | 0.06 |
| MB | 7-8 | -2.53 | -2.50 | 4.66 | 4.65 | 0.01 |
| MB | 8-1 | -4.74 | -4.84 | 2.37 | 2.31 | -0.08 |

Fig. 17. Table keeping track of MB mulipoles *b3, b4, b5* per sector and per beam

In this case, the corresponding entries for beam 1 and 2 are updated. These values are based on the deterministic part of the errors, beam screen included. We need to store the correction table since it is needed for other simulations, like the *geometry* error source, for which we would not make any field quality error estimates.

The correction table is output as a .madx script, once for each iteration, if and only if:

- The option *Do not power corrector magnets* is disabled
- At least one sector must be selected (Fig. 2)
- The magnet type MB and one of the *b3, b4, b5* multipoles are selected

Equations 9 to 11 show the computation of the correction demand, where $k$ is the multipole order to be corrected (3 for sextupole, …), $B_c$ is the field of the correctors, $B_{mb}$ the nominal field of the main dipoles (both in T), $E_{mb}$ is the error (units) of the multipole to correct, $n$ is the number of magnets (main dipoles or correctors) on the same power supply, and $l$ is the magnetic length:

$$B_c(k) = -10^{-4} B_{mb}\, E(k)_{mb} \frac{n_{mb} l_{mb}}{n_c l_c} [T] \tag{9}$$

The quantity $G$ is computed from the field using the standard expression.

$$G_c(k) = \frac{B_c(k)}{R_{ref}^{\,k-1}} \quad [T \cdot m^{1-k}] \tag{10}$$

If the modulus of the needed $G$ is larger than the nominal $G$, we have exceeded the correction capacity and we use the nominal $G$ instead. Eq. (11) gives the normalized strength used by MAD-X given the physical gradient. Fig. 18 shows an example of the WISE output file for powering the spool pieces

$$K_{mad}(k) = (k-1)!\frac{G_c(k)}{B_{mb}\rho_0} \quad [m^{-k}] \tag{11}$$

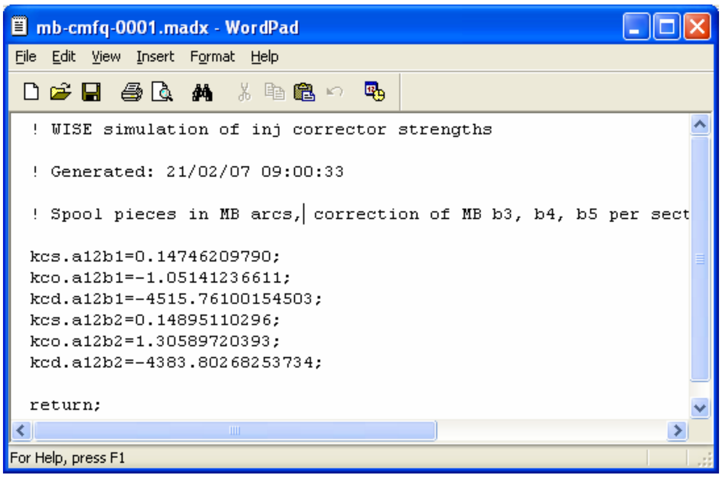


```
! WISE simulation of inj corrector strengths

! Generated: 21/02/07 09:00:33

! Spool pieces in MB arcs, correction of MB b3, b4, b5 per sect

kcs.a12b1=0.14746209790;
kco.a12b1=-1.05141236611;
kcd.a12b1=-4515.76100154503;
kcs.a12b2=0.14895110296;
kco.a12b2=1.30589720393;
kcd.a12b2=-4383.80268253734;

return;
```

Fig. 18. The MAD-X script for powering the spool pieces

### 3.4 Log file of error generation in the sheet MAD FQ errors

The column *error details* in the sheet *MAD FQ errors* contains indication about how WISE computed the field quality errors, and which values have been used for drawing the uncertainties. It can be useful in a debugging phase or in case of doubts. The power error source writes a description like this:

*POWER=value*

To illustrate the field quality errors, let us take an example from simulation of MB errors. Suppose you see the text:

*FQ:ITF=WC+UNCERT{CLASS G+R+S=0.10 DRAW R=0.60}*

This means the error estimate for the main field (integrated transfer function) is based upon "warm-to-cold" extrapolation. The total uncertainty for the MB magnet type was 0.1 units, whilst the individual uncertainty was 0.6 units. See 3.1.8 for symbol definition. The next column could typically say:

*FQ:MUL=WC*

This means the multipoles were also generated from "warm-to-cold" extrapolation. Writing details for each multipole would be overwhelming. By inspecting the measurement data and statistics you see how WISE arrived exactly at the result. There are measurements where the main field is measured at "warm" whilst the multipoles have been measured at "cold". The computation method (as given by equations 1 to 5) is chosen independently for main field and multipoles according to availability. The last column says

*COMMON_POWER_ERROR=value*

This is the common, deterministic error in the main field for magnets sharing power supply.

### 3.5 WISE output format for field quality errors

As explained in section 2.4, output results are written in MAD-X TFS table format. The TFS table is an ASCII file as shown in Fig. 19. The top of the table contains header information about when the simulation took place and which options were active. Next follows data for all the magnets that can be simulated in WISE. There is one aperture for each row. The table is a sparse matrix where only magnets simulated have non-zero errors. All field errors are relative (units of the main field).

The name is the official LHC optical id with one subtle difference. The official convention for optics ids is beam-centric. The LHC optics sequence use suffices *.B1* or *.B2* for dual aperture magnets, or magnets carrying only 1 beam, and no suffix for magnets carrying both beams. The WISE output uses instead *.V1* and *.V2* suffices which means aperture 1 (left external) and 2 (right internal) as seen from the connection side (CS). The mapping to beams is done by the .madx scripts processing the TFS table.

The field errors are expressed from a reference frame seen from the CS-side of the cryostat [8]. Some insertion magnets are π-rotated around the vertical y-axis when installed in the tunnel. The MAD-X script processing the .TFS table therefore flips the sign of multipoles accordingly. These conventions must be strictly adhered to avoid sign problems inside MAD-X. WISE needs to estimate field errors for both apertures since some errors are accounted for per beam. Therefore it also needs to map between apertures and beams. Fig. 20 shows the lookup table.

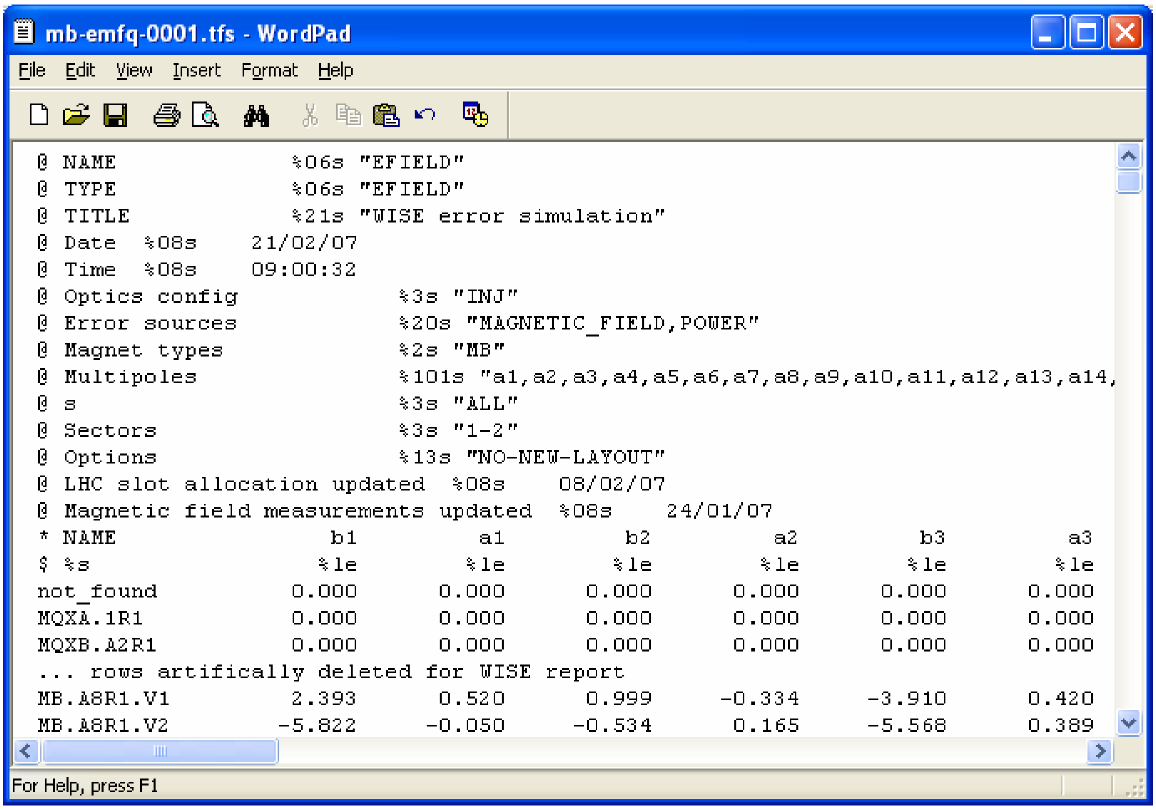


```
@ NAME                %06s "EFIELD"
@ TYPE                %06s "EFIELD"
@ TITLE               %21s "WISE error simulation"
@ Date  %08s    21/02/07
@ Time  %08s    09:00:32
@ Optics config                %3s "INJ"
@ Error sources                %20s "MAGNETIC_FIELD,POWER"
@ Magnet types                 %2s "MB"
@ Multipoles                   %101s "a1,a2,a3,a4,a5,a6,a7,a8,a9,a10,a11,a12,a13,a14,
@ s                            %3s "ALL"
@ Sectors                      %3s "1-2"
@ Options                      %13s "NO-NEW-LAYOUT"
@ LHC slot allocation updated  %08s    08/02/07
@ Magnetic field measurements updated  %08s    24/01/07
* NAME                  b1         a1         b2         a2         b3         a3
$ %s                   %le        %le        %le        %le        %le        %le
not_found            0.000      0.000      0.000      0.000      0.000      0.000
MQXA.1R1             0.000      0.000      0.000      0.000      0.000      0.000
MQXB.A2R1            0.000      0.000      0.000      0.000      0.000      0.000
... rows artifically deleted for WISE report
MB.A8R1.V1           2.393      0.520      0.999     -0.334     -3.910      0.420
MB.A8R1.V2          -5.822     -0.050     -0.534      0.165     -5.568      0.389
```

Fig. 19. TFS table for field quality errors

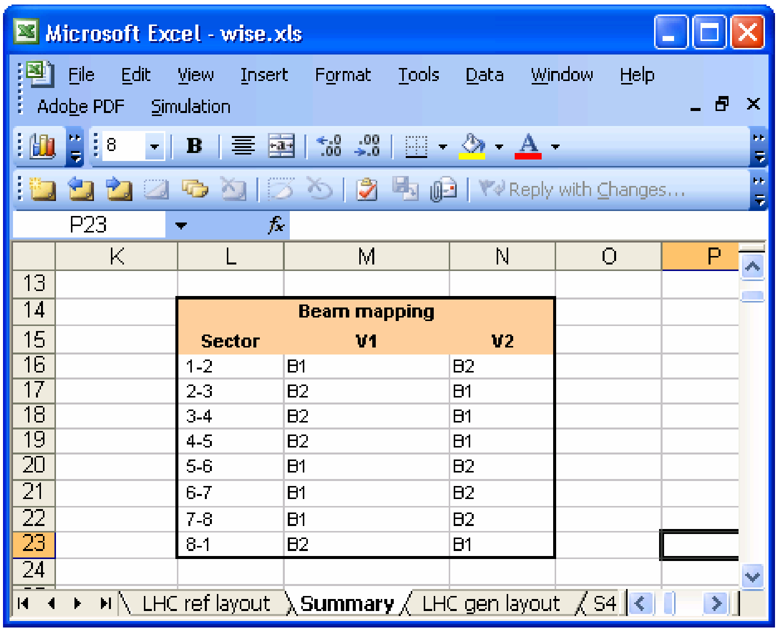


Fig. 20. Lookup table mapping apertures and beams in the *Summary* sheet.

### 3.6 Specified errors

The option in Fig. 4 *Use specified errors* is a little used option, although it can be useful. If selected, the table with specified errors is used blindly for all magnets selected. Measurements and uncertainty are ignored. The intention of this is for some simple *what if* scenarios. Example: Suppose somebody asked you: What beta-beating would result from *Q2.R1* having a main field error of 42 units? The solution would be to select magnetic field as error source, magnet type MQXB and s-coordinate range 30-44 and finally fill in the error table. Hint: See sheet *LHC ref layout* to find the derived data.

### 3.7 Miscellaneous about processing of field quality measurements

All the “cold” measurements are loaded from the AT/MTM database [9], except for the *MBXW* separation dipoles where data manually were extracted from MTF [10]. The “warm” measurements for the *MB* and *MQ* in the arcs are from AT/MCS [11]. The “warm” measurements for *MQM* insertion magnets are automatically downloaded from property sheets in MTF. The “warm” measurements for *MQS*, *MQT* and *MQTL* magnets are downloaded from AT/MEL [12].

In order to make the download of measurement data data-driven, a table is used for “cold” measurements to fetch the appropriate data (Fig. 21). Each magnet type has many data entries and the selection of representative data for injection and collision cycles remains a non-trivial issue.

Only field integral errors are used. This is fine for the LHC thick lens model where each magnet is represented by one optical element. However, the thin lens model operates with slices. That is, magnets where the optics functions change rapidly inside are represented by several optical elements. Therefore a more accurate thin lens simulation would require a field model where the field quality is a function of longitudinal position. This is not yet available.

The “cold” measurements sometimes miss the main field component. But cold measurements are precious (not abundant in nature) so we also use “cold” measurements with incomplete data inside WISE at the cost of some more perturbed code.

The field quality measurement data stored in WISE uses the convention in [8]. Most of the data is already in this form when downloading. The exceptions are:

- "Warm" *MQM* data in MTF was measured "upside-down" compared to as assembled.

- The skew quadrupoles *MQS* were measured as normal quadrupoles but rotated π/4 when installed

When writing this report (1st quarter 2007) some data validation of magnets remain [13]. There is still some uncertainty concerning what happened to corrector magnets when installed concerning rotations. For a simple case like MQS, there is for example the possibility to rotate + or - π/4. No "cold" measurements of the MQSX magnets are yet in the database and "warm-to-cold" correlations are needed for corrector magnets.

There is a little used option in Fig. 4 which applies to the MQ data. *Use MQ measurements without permeability corrections.* Although this option might never be used again, we will just mention it. The "warm" measurements of MQ with low current are originally perturbed by collar permeability. This effect fortunately disappears at "cold". It has later on been possible to correct the "warm" data for this effect based upon a model using the sensitivity to collar-permeability. This contributes to more spread in the "warm" data as well as the "warm-to-cold" correlations. If this option is selected, MQ "warm" data without permeability-correction will be downloaded when updating measurements. If you do this, be aware that the statistics table in Fig. 9 needs to be updated *manually* concerning the MQ entries. This allows the "what if" scenarios: (a) that permeability is not the cause of the production spread, (b) that the effect does not disappear at "cold".

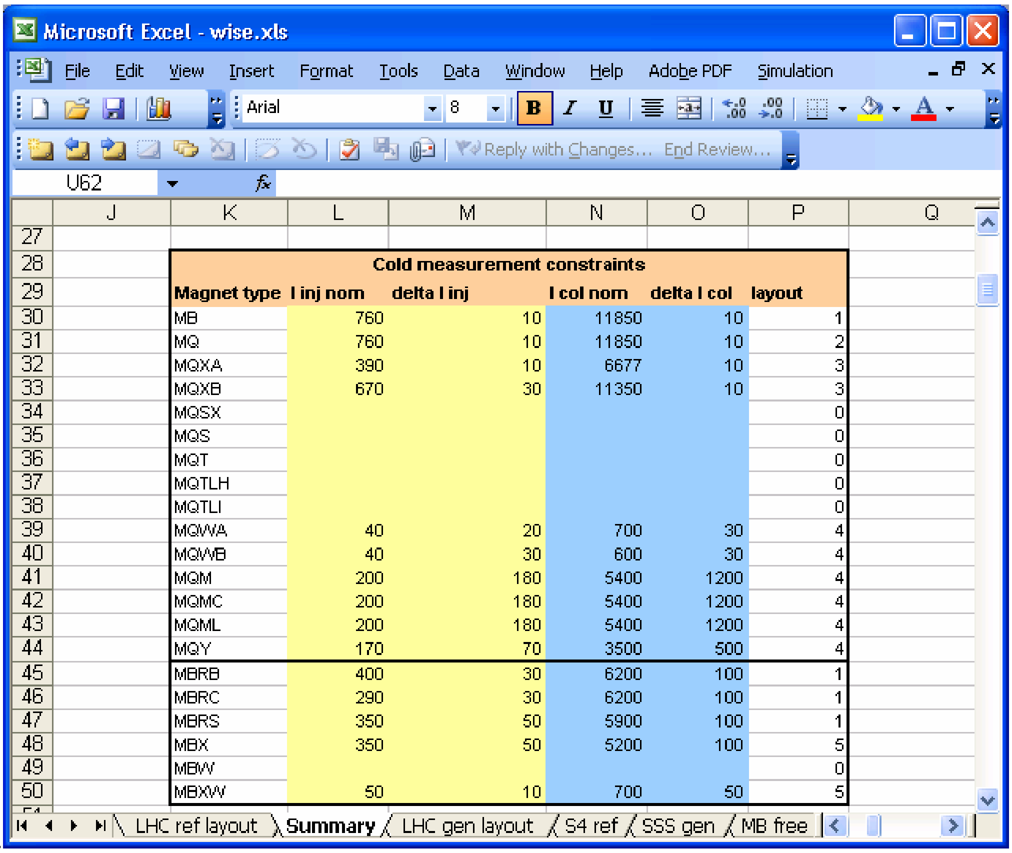

Cold measurement constraints

| Magnet type | I inj nom | delta I inj | I col nom | delta I col | layout |
|---|---|---|---|---|---|
| MB | 760 | 10 | 11850 | 10 | 1 |
| MQ | 760 | 10 | 11850 | 10 | 2 |
| MQXA | 390 | 10 | 6677 | 10 | 3 |
| MQXB | 670 | 30 | 11350 | 10 | 3 |
| MQSX | | | | | 0 |
| MQS | | | | | 0 |
| MQT | | | | | 0 |
| MQTLH | | | | | 0 |
| MQTLI | | | | | 0 |
| MQWA | 40 | 20 | 700 | 30 | 4 |
| MQWB | 40 | 30 | 600 | 30 | 4 |
| MQM | 200 | 180 | 5400 | 1200 | 4 |
| MQMC | 200 | 180 | 5400 | 1200 | 4 |
| MQML | 200 | 180 | 5400 | 1200 | 4 |
| MQY | 170 | 70 | 3500 | 500 | 4 |
| MBRB | 400 | 30 | 6200 | 100 | 1 |
| MBRC | 290 | 30 | 6200 | 100 | 1 |
| MBRS | 350 | 50 | 5900 | 100 | 1 |
| MBX | 350 | 50 | 5200 | 100 | 5 |
| MBW | | | | | 0 |
| MBXW | 50 | 10 | 700 | 50 | 5 |

Fig. 21. The helper table for selecting measurements as function of current

Another issue is that we only have field-integrals for the entire cryostat for some "cold" measurements where the cryostats contains two main magnets inside. To be more precise: Some MQY and MQXB magnets. It would have been more precise for MAD-X to have them per magnet. This is particular important where the optics parameters change quickly (like beta function or phase advance). The observant WISE user will therefore notice that in the sheets MQY FQ and MQXB FQ the column with magnet number is empty, but the cold mass id identifying the cryostat is present.

The issues in this section should improve as we approach LHC commissioning and the FiDeL [3] project progresses.

## 4. GEOMETRY ERRORS

The misalignment of magnets both in the transversal and longitudinal plane causes degradation of field quality. For example misaligned *MCS* (sextupolar) spool pieces generates a quadrupole term to first order, and misalignment of quadrupoles causes errors in the closed orbit. MAD-X takes care of misalignment-to-field calculations, and WISE only provides estimates for the spatial misalignments and rotations as specified by the MAD-X [1] function *Ealign*.

Since part of the errors induce feed-down in the correctors, these magnets have to be powered to see some effect in MAD-X. In section 3.3 we discussed the powering of the MB spool pieces driven by field errors in the MB main dipoles. These are the only corrector magnets where WISE by default proposes strengths. If you want to observe geometry errors from other types of corrector magnets you must modify the MAD-X template scripts from WISE.

The simulation of geometry errors are driven by two sources of errors: magnet geometry errors and cryostat alignment errors in the LHC tunnel. The first source is due to misplacement of individual magnets during assembly into cryostat. The second source is what happens to the cryostat afterwards, before and after installation into the tunnel.

Let $D$ be the geometry error vector. $m$ denotes a magnet and $c$ a cryostat. We have

$$\vec{D}(i) = \vec{D}_m(i) + \vec{D}_c(i) \tag{12}$$

The spatial errors are conveniently expressed in *mm* and angles in *mrad*. The components of $D$ are:

- $\Delta dx$, $\Delta dy$ for transverse displacements
- $\Delta s$ for longitudinal displacement
- $\psi$ for field angle, i.e. a rotation around the $s$-axis.
- $\theta$ for rotation around $y$-axis
- $\varphi$ for rotation around $x$-axis

The coordinate system is right-handed with counter-clockwise angles. The $x$ and $y$ axis are defined in [8], i.e. seeing the cryostat from the CS connection side. The s-axis is the bent trajectory of beam 1 (clock-wise). The Greek letters for angles are as defined in MAD-X [1]. The same coordinate system is used for both beams whereas in MAD-X it is different for the two.

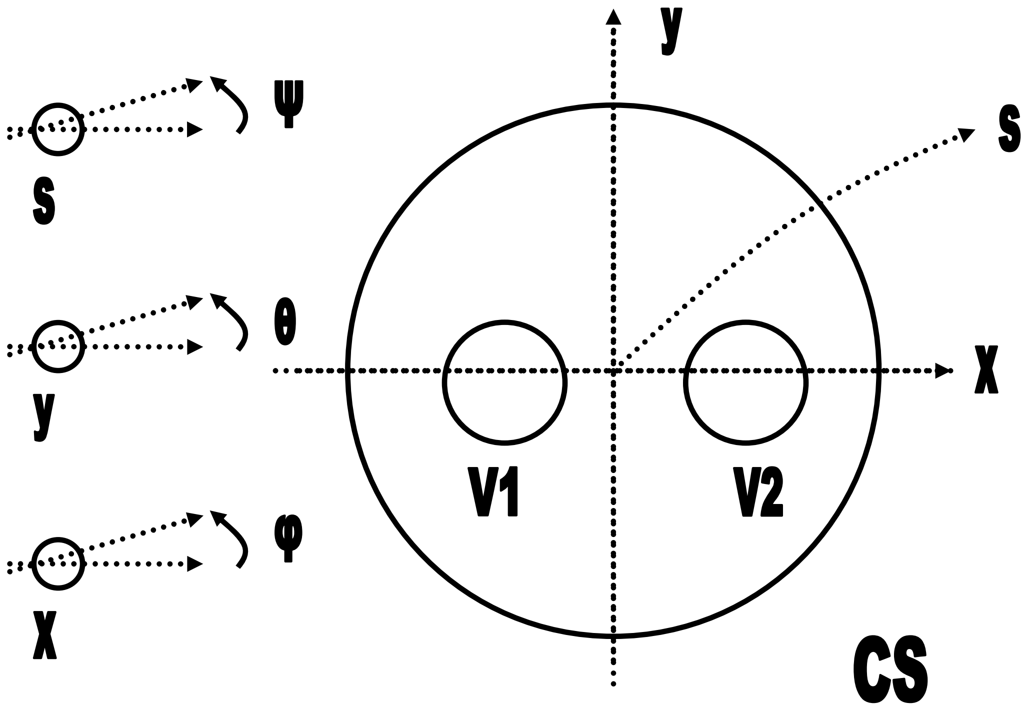

Fig. 22. The WISE coordinate system

### 4.1 Measurement data

The measurement data is extracted from the AT/MCS geometry database [11].

For the main bending one has (see MB Geo sheet, Fig. 23)

- *cmid* and *ap* denoting the cryostat number and the aperture.
- *ψ,* i.e. the angle of the main field in each aperture with respect to the mid-plane. This is measured for a fraction of magnets at room temperature (except Firm2, where no measurements are available), at the end of the assembly process in the manufacturers. It is downloaded from the magnetic measurement database.
- *dx, dy, ds* are the installation shifts. All magnets are measured after "cold test" at room temperature (WP08); this measurement is used to find the cryostat or magnet axes. The cryostat or magnet is installed by default on the ideal orbit. Therefore these shifts are zero by default. Small shifts (of the order of 0.1 mm)may be applied to maximize the mechanical aperture. Please note that these shifts have to be taken into account for all magnets inside a given cryostat.
- MCS *dx, dy* this is the offset between the main dipole axes and the position of the MCS spool pieces, measured at WP08.
- MCDO *dx, dy* this is the offset between the main dipole axes and the position of the MCDO spool pieces, measured at WP08.

For the short straight sections the sheet is similar to the MB. The only difference is that a column is added for the transverse offset of the MQ with respect to the cryostat axis (see Fig. 24). In fact, the cryostat axes are evaluated through a fit that covers all the SSS and not only the MQ part, and therefore the MQ position is not zero by default. The transverse offsets between the cryostat axes and the correctors are given, as for the *MB Geo*.

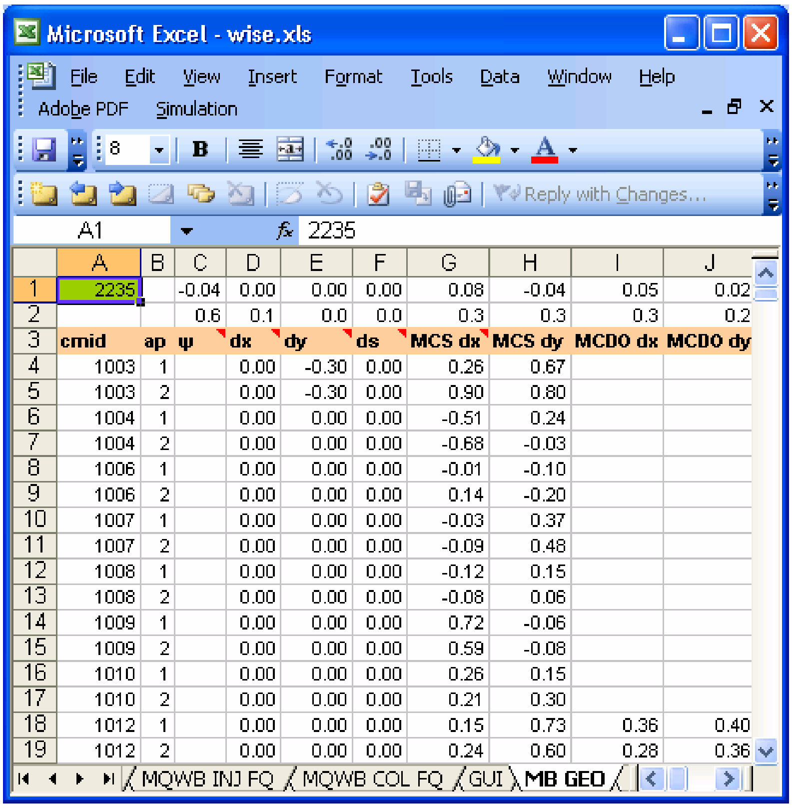
Microsoft Excel - wise.xls

File Edit View Insert Format Tools Data Window Help Adobe PDF Simulation

A1 2235

| | A | B | C | D | E | F | G | H | I | J |
|---|---|---|---|---|---|---|---|---|---|---|
| 1 | 2235 | | -0.04 | 0.00 | 0.00 | 0.00 | 0.08 | -0.04 | 0.05 | 0.02 |
| 2 | | | 0.6 | 0.1 | 0.0 | 0.0 | 0.3 | 0.3 | 0.3 | 0.2 |
| 3 | cmid | ap | ψ | dx | dy | ds | MCS dx | MCS dy | MCDO dx | MCDO dy |
| 4 | 1003 | 1 | | 0.00 | -0.30 | 0.00 | 0.26 | 0.67 | | |
| 5 | 1003 | 2 | | 0.00 | -0.30 | 0.00 | 0.90 | 0.80 | | |
| 6 | 1004 | 1 | | 0.00 | 0.00 | 0.00 | -0.51 | 0.24 | | |
| 7 | 1004 | 2 | | 0.00 | 0.00 | 0.00 | -0.68 | -0.03 | | |
| 8 | 1006 | 1 | | 0.00 | 0.00 | 0.00 | -0.01 | -0.10 | | |
| 9 | 1006 | 2 | | 0.00 | 0.00 | 0.00 | 0.14 | -0.20 | | |
| 10 | 1007 | 1 | | 0.00 | 0.00 | 0.00 | -0.03 | 0.37 | | |
| 11 | 1007 | 2 | | 0.00 | 0.00 | 0.00 | -0.09 | 0.48 | | |
| 12 | 1008 | 1 | | 0.00 | 0.00 | 0.00 | -0.12 | 0.15 | | |
| 13 | 1008 | 2 | | 0.00 | 0.00 | 0.00 | -0.08 | 0.06 | | |
| 14 | 1009 | 1 | | 0.00 | 0.00 | 0.00 | 0.72 | -0.06 | | |
| 15 | 1009 | 2 | | 0.00 | 0.00 | 0.00 | 0.59 | -0.08 | | |
| 16 | 1010 | 1 | | 0.00 | 0.00 | 0.00 | 0.26 | 0.15 | | |
| 17 | 1010 | 2 | | 0.00 | 0.00 | 0.00 | 0.21 | 0.30 | | |
| 18 | 1012 | 1 | | 0.00 | 0.00 | 0.00 | 0.15 | 0.73 | 0.36 | 0.40 |
| 19 | 1012 | 2 | | 0.00 | 0.00 | 0.00 | 0.24 | 0.60 | 0.28 | 0.36 |

MQWB INJ FQ / MQWB COL FQ / GUI / MB GEO

Fig. 23. The sheet *MB GEO* with geometry measurements

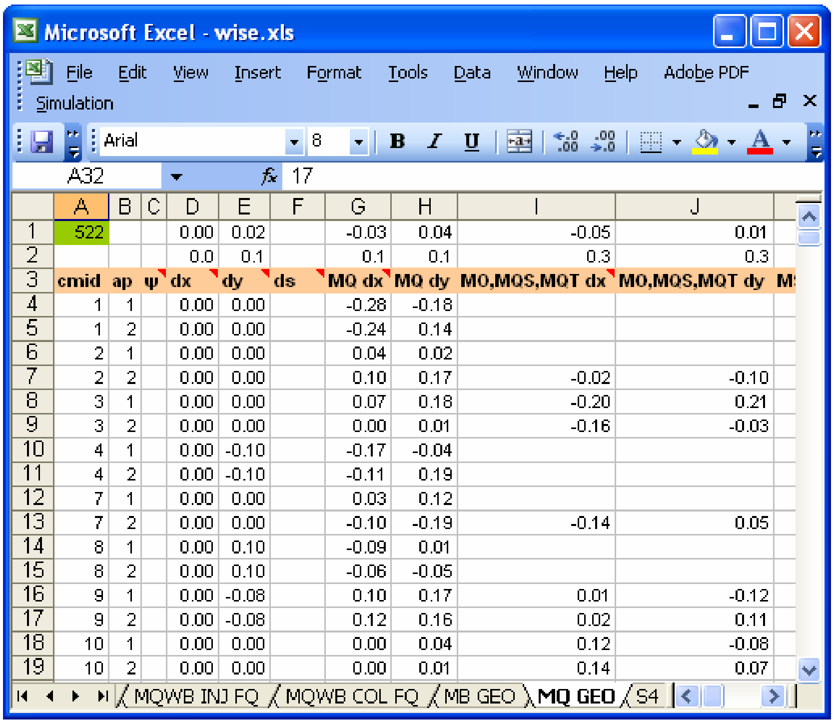
Microsoft Excel - wise.xls

File Edit View Insert Format Tools Data Window Help Adobe PDF Simulation

A32 17

| | A | B | C | D | E | F | G | H | I | J |
|---|---|---|---|---|---|---|---|---|---|---|
| 1 | 522 | | | 0.00 | 0.02 | | -0.03 | 0.04 | -0.05 | 0.01 |
| 2 | | | | 0.0 | 0.1 | | 0.1 | 0.1 | 0.3 | 0.3 |
| 3 | cmid | ap | ψ | dx | dy | ds | MQ dx | MQ dy | MO,MQS,MQT dx | MO,MQS,MQT dy |
| 4 | 1 | 1 | | 0.00 | 0.00 | | -0.28 | -0.18 | | |
| 5 | 1 | 2 | | 0.00 | 0.00 | | -0.24 | 0.14 | | |
| 6 | 2 | 1 | | 0.00 | 0.00 | | 0.04 | 0.02 | | |
| 7 | 2 | 2 | | 0.00 | 0.00 | | 0.10 | 0.17 | -0.02 | -0.10 |
| 8 | 3 | 1 | | 0.00 | 0.00 | | 0.07 | 0.18 | -0.20 | 0.21 |
| 9 | 3 | 2 | | 0.00 | 0.00 | | 0.00 | 0.01 | -0.16 | -0.03 |
| 10 | 4 | 1 | | 0.00 | -0.10 | | -0.17 | -0.04 | | |
| 11 | 4 | 2 | | 0.00 | -0.10 | | -0.11 | 0.19 | | |
| 12 | 7 | 1 | | 0.00 | 0.00 | | 0.03 | 0.12 | | |
| 13 | 7 | 2 | | 0.00 | 0.00 | | -0.10 | -0.19 | -0.14 | 0.05 |
| 14 | 8 | 1 | | 0.00 | 0.10 | | -0.09 | 0.01 | | |
| 15 | 8 | 2 | | 0.00 | 0.10 | | -0.06 | -0.05 | | |
| 16 | 9 | 1 | | 0.00 | -0.08 | | 0.10 | 0.17 | 0.01 | -0.12 |
| 17 | 9 | 2 | | 0.00 | -0.08 | | 0.12 | 0.16 | 0.02 | 0.11 |
| 18 | 10 | 1 | | 0.00 | 0.00 | | 0.00 | 0.04 | 0.12 | -0.08 |
| 19 | 10 | 2 | | 0.00 | 0.00 | | 0.00 | 0.01 | 0.14 | 0.07 |

MQWB INJ FQ / MQWB COL FQ / MB GEO / MQ GEO / S4

Fig. 24. The sheet *MQ GEO* with geometry measurements

The sheet *S4 GEO* contains the insertion quadrupoles whilst *X GEO* contains some of the single aperture magnets around the IPs, namely the inner triplets and separation dipoles. WISE currently has only field angle measurements for MB. Data is currently missing for some types: Warm magnet assemblies, MBX cryostat and the MQSX corrector magnet in the inner triplet.

### 4.2 Simulation of the alignment errors

Three different effects are considered.

- Impact of transport to the tunnel from WP08 to installation. A few tens of magnets have been measured in the tunnel. Please note that in this case only the ends can be measured, since the beam screen is inside the magnet. One has to make an hypothesis on the movement between the ends. We assume that only the ends are moving, i.e. that this affects only the MB spool pieces. For the straight magnets we assume that there is no effect.

- Precision of alignment of the cryostat in the tunnel. It is simulated using a Gaussian with zero average and given values for the standard deviations.

- Movements of the cryostat in the tunnel during one year lifetime of the machine. These movements are estimated on the basis of the experience acquired with LEP.

The average and standard deviation of the geometric measurements can be found in the *Summary* sheet (see Fig. 25). Each class of magnets have 6 rows for the *D* vector, and describes several magnet types. The table is used to generate missing measurements. Three more tables contain the expected average and standard deviation used to generate the above quoted uncertainties (transportation, alignment, and movements).

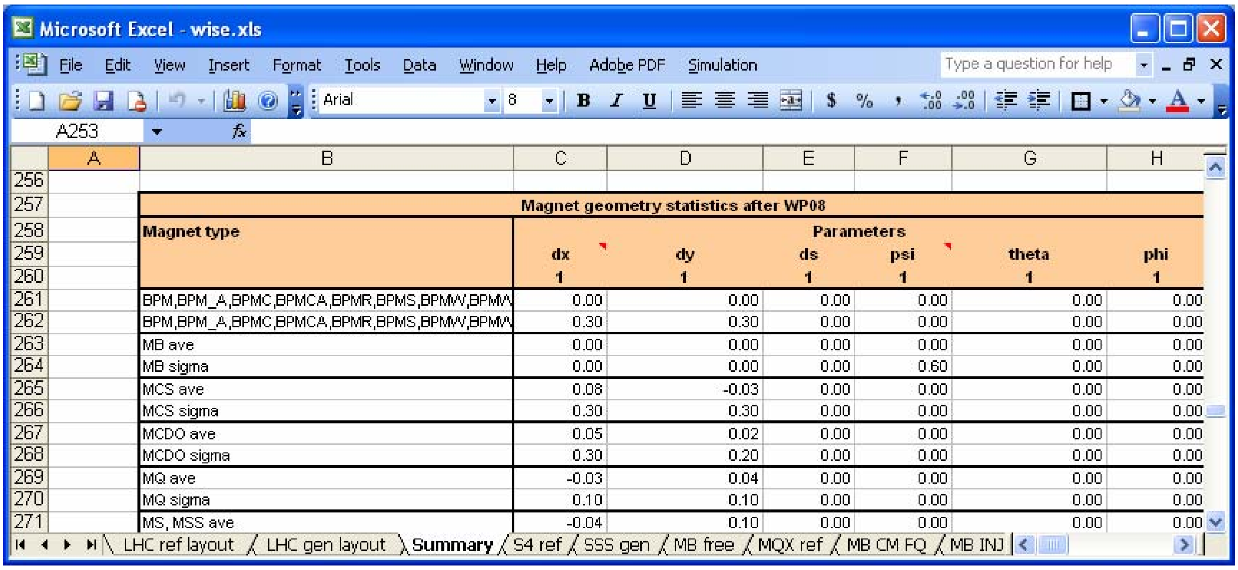


| | A | B | C | D | E | F | G | H |
|---|---|---|---|---|---|---|---|---|
| 256 | | | | | | | | |
| 257 | | Magnet geometry statistics after WP08 | | | | | | |
| 258 | | Magnet type | Parameters | | | | | |
| 259 | | | dx | dy | ds | psi | theta | phi |
| 260 | | | 1 | 1 | 1 | 1 | 1 | 1 |
| 261 | | BPM,BPM_A,BPMC,BPMCA,BPMR,BPMS,BPMW,BPMW | 0.00 | 0.00 | 0.00 | 0.00 | 0.00 | 0.00 |
| 262 | | BPM,BPM_A,BPMC,BPMCA,BPMR,BPMS,BPMW,BPMW | 0.30 | 0.30 | 0.00 | 0.00 | 0.00 | 0.00 |
| 263 | | MB ave | 0.00 | 0.00 | 0.00 | 0.00 | 0.00 | 0.00 |
| 264 | | MB sigma | 0.00 | 0.00 | 0.00 | 0.60 | 0.00 | 0.00 |
| 265 | | MCS ave | 0.08 | -0.03 | 0.00 | 0.00 | 0.00 | 0.00 |
| 266 | | MCS sigma | 0.30 | 0.30 | 0.00 | 0.00 | 0.00 | 0.00 |
| 267 | | MCDO ave | 0.05 | 0.02 | 0.00 | 0.00 | 0.00 | 0.00 |
| 268 | | MCDO sigma | 0.30 | 0.20 | 0.00 | 0.00 | 0.00 | 0.00 |
| 269 | | MQ ave | -0.03 | 0.04 | 0.00 | 0.00 | 0.00 | 0.00 |
| 270 | | MQ sigma | 0.10 | 0.10 | 0.00 | 0.00 | 0.00 | 0.00 |
| 271 | | MS, MSS ave | -0.04 | 0.10 | 0.00 | 0.00 | 0.00 | 0.00 |

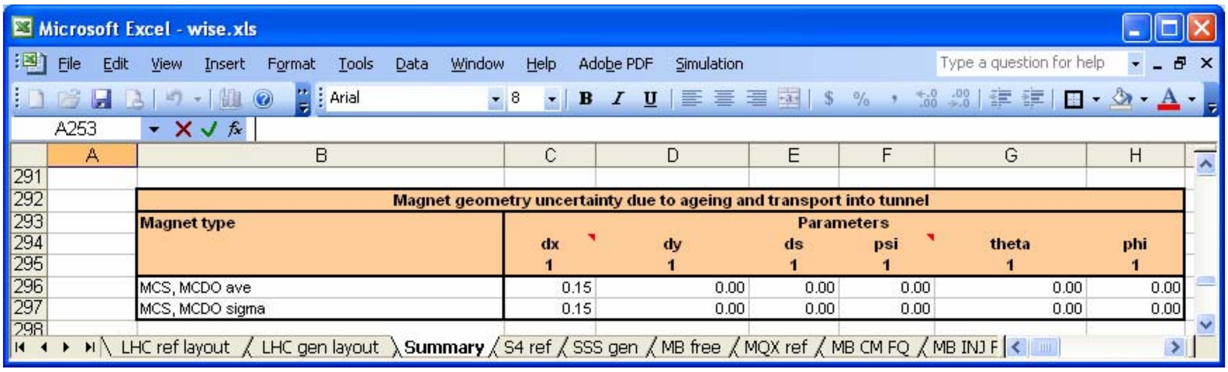

| Magnet geometry uncertainty due to ageing and transport into tunnel | | | | | | |
|---|---|---|---|---|---|---|
| Magnet type | Parameters | | | | | |
| | dx | dy | ds | psi | theta | phi |
| | 1 | 1 | 1 | 1 | 1 | 1 |
| MCS, MCDO ave | 0.15 | 0.00 | 0.00 | 0.00 | 0.00 | 0.00 |
| MCS, MCDO sigma | 0.15 | 0.00 | 0.00 | 0.00 | 0.00 | 0.00 |

Fig. 25. The tables for Geometry statistics (single magnets) in *Summary* sheet

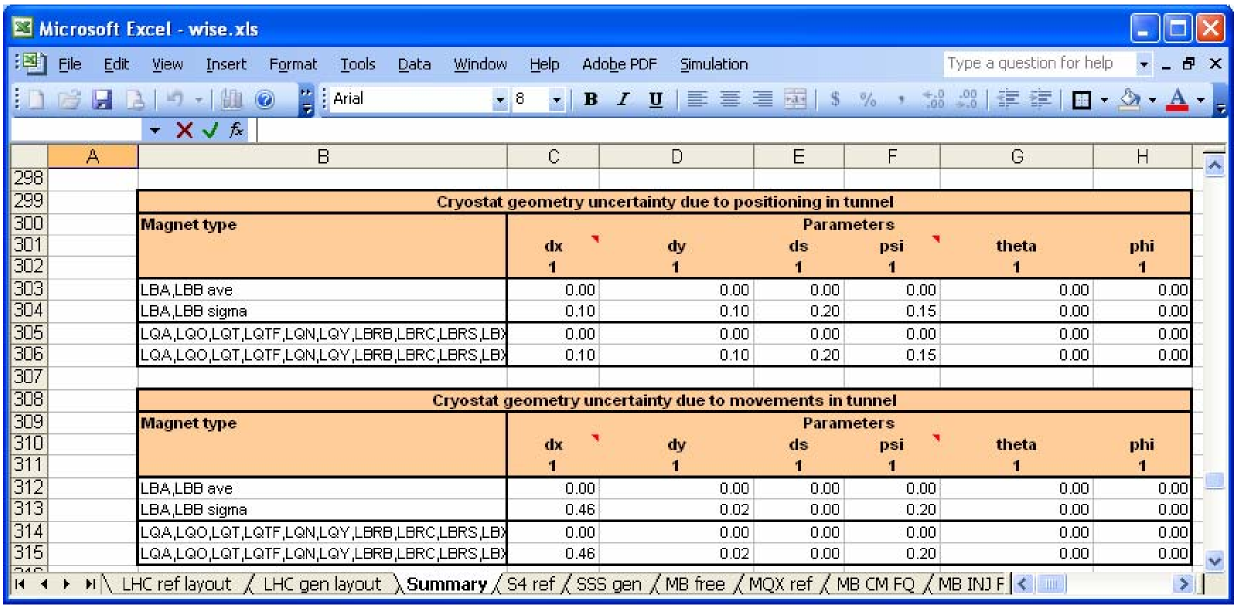

| Cryostat geometry uncertainty due to positioning in tunnel | | | | | | |
|---|---|---|---|---|---|---|
| Magnet type | Parameters | | | | | |
| | dx | dy | ds | psi | theta | phi |
| | 1 | 1 | 1 | 1 | 1 | 1 |
| LBA,LBB ave | 0.00 | 0.00 | 0.00 | 0.00 | 0.00 | 0.00 |
| LBA,LBB sigma | 0.10 | 0.10 | 0.20 | 0.15 | 0.00 | 0.00 |
| LQA,LQO,LQT,LQTF,LQN,LQY,LBRB,LBRC,LBRS,LBX | 0.00 | 0.00 | 0.00 | 0.00 | 0.00 | 0.00 |
| LQA,LQO,LQT,LQTF,LQN,LQY,LBRB,LBRC,LBRS,LBX | 0.10 | 0.10 | 0.20 | 0.15 | 0.00 | 0.00 |

| Cryostat geometry uncertainty due to movements in tunnel | | | | | | |
|---|---|---|---|---|---|---|
| Magnet type | Parameters | | | | | |
| | dx | dy | ds | psi | theta | phi |
| | 1 | 1 | 1 | 1 | 1 | 1 |
| LBA,LBB ave | 0.00 | 0.00 | 0.00 | 0.00 | 0.00 | 0.00 |
| LBA,LBB sigma | 0.46 | 0.02 | 0.00 | 0.20 | 0.00 | 0.00 |
| LQA,LQO,LQT,LQTF,LQN,LQY,LBRB,LBRC,LBRS,LBX | 0.00 | 0.00 | 0.00 | 0.00 | 0.00 | 0.00 |
| LQA,LQO,LQT,LQTF,LQN,LQY,LBRB,LBRC,LBRS,LBX | 0.46 | 0.02 | 0.00 | 0.20 | 0.00 | 0.00 |

Fig. 26. The tables for Geometry statistics (cryostats) in *Summary* sheet

### 4.3 WISE output format for geometry errors

The geometry errors are written into the sheet *MAD GEO errors* during simulation. Thereafter they are written into MAD-X .TFS tables. We first describe the intermediate format of the Excel sheet briefly as it is convenient for debugging and data validation. Fig. 27 shows the top of the sheet. The sheets buffers one iteration of the simulation for both beams. Each row contains sufficient information to compute the alignment errors for MAD-X.

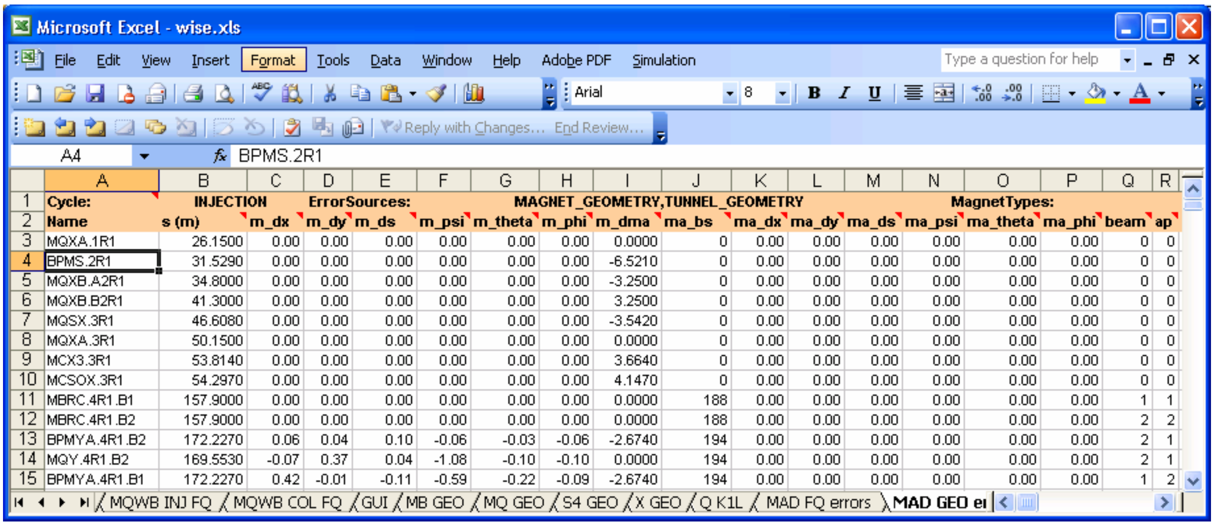

| Cycle: | INJECTION | | ErrorSources: | | | MAGNET_GEOMETRY,TUNNEL_GEOMETRY | | | | | | | MagnetTypes: | | | | |
|---|---|---|---|---|---|---|---|---|---|---|---|---|---|---|---|---|---|
| Name | s (m) | m_dx | m_dy | m_ds | m_psi | m_theta | m_phi | m_dma | ma_bs | ma_dx | ma_dy | ma_ds | ma_psi | ma_theta | ma_phi | beam | ap |
| MQXA.1R1 | 26.1500 | 0.00 | 0.00 | 0.00 | 0.00 | 0.00 | 0.00 | 0.0000 | 0 | 0.00 | 0.00 | 0.00 | 0.00 | 0.00 | 0.00 | 0 | 0 |
| BPMS.2R1 | 31.5290 | 0.00 | 0.00 | 0.00 | 0.00 | 0.00 | 0.00 | -6.5210 | 0 | 0.00 | 0.00 | 0.00 | 0.00 | 0.00 | 0.00 | 0 | 0 |
| MQXB.A2R1 | 34.8000 | 0.00 | 0.00 | 0.00 | 0.00 | 0.00 | 0.00 | -3.2500 | 0 | 0.00 | 0.00 | 0.00 | 0.00 | 0.00 | 0.00 | 0 | 0 |
| MQXB.B2R1 | 41.3000 | 0.00 | 0.00 | 0.00 | 0.00 | 0.00 | 0.00 | 3.2500 | 0 | 0.00 | 0.00 | 0.00 | 0.00 | 0.00 | 0.00 | 0 | 0 |
| MQSX.3R1 | 46.6080 | 0.00 | 0.00 | 0.00 | 0.00 | 0.00 | 0.00 | -3.5420 | 0 | 0.00 | 0.00 | 0.00 | 0.00 | 0.00 | 0.00 | 0 | 0 |
| MQXA.3R1 | 50.1500 | 0.00 | 0.00 | 0.00 | 0.00 | 0.00 | 0.00 | 0.0000 | 0 | 0.00 | 0.00 | 0.00 | 0.00 | 0.00 | 0.00 | 0 | 0 |
| MCX3.3R1 | 53.8140 | 0.00 | 0.00 | 0.00 | 0.00 | 0.00 | 0.00 | 3.6640 | 0 | 0.00 | 0.00 | 0.00 | 0.00 | 0.00 | 0.00 | 0 | 0 |
| MCSOX.3R1 | 54.2970 | 0.00 | 0.00 | 0.00 | 0.00 | 0.00 | 0.00 | 4.1470 | 0 | 0.00 | 0.00 | 0.00 | 0.00 | 0.00 | 0.00 | 0 | 0 |
| MBRC.4R1.B1 | 157.9000 | 0.00 | 0.00 | 0.00 | 0.00 | 0.00 | 0.00 | 0.0000 | 188 | 0.00 | 0.00 | 0.00 | 0.00 | 0.00 | 0.00 | 1 | 1 |
| MBRC.4R1.B2 | 157.9000 | 0.00 | 0.00 | 0.00 | 0.00 | 0.00 | 0.00 | 0.0000 | 188 | 0.00 | 0.00 | 0.00 | 0.00 | 0.00 | 0.00 | 2 | 2 |
| BPMYA.4R1.B2 | 172.2270 | 0.06 | 0.04 | 0.10 | -0.06 | -0.03 | -0.06 | -2.6740 | 194 | 0.00 | 0.00 | 0.00 | 0.00 | 0.00 | 0.00 | 2 | 1 |
| MQY.4R1.B2 | 169.5530 | -0.07 | 0.37 | 0.04 | -1.08 | -0.10 | -0.10 | 0.0000 | 194 | 0.00 | 0.00 | 0.00 | 0.00 | 0.00 | 0.00 | 2 | 1 |
| BPMYA.4R1.B1 | 172.2270 | 0.42 | -0.01 | -0.11 | -0.59 | -0.22 | -0.09 | -2.6740 | 194 | 0.00 | 0.00 | 0.00 | 0.00 | 0.00 | 0.00 | 1 | 2 |

Fig. 27. The sheet *MQ GEO errors* used as intermediate output

- The *Name* column is the optics id used by MAD-X. It includes the beam number.

- The column *s* is the s-coordinate clockwise. Recall that we defined the coordinate system in WISE to be the same for both beams. The s-coordinate is generated from the *LHC ref sheet.* This sheet shows the cryostats as installed.

- The vector represented by 6 columns with names starting with *m_* gives the displacement for single magnets.

- The column *m_dma* is the *s* distance from the mid-point of cryostat to middle of this magnet. We have somewhat artificially defined the s-origin inside a cryostat to be in the middle between the first and last main magnet.

- The column *m_bs* is the beam separation, unsigned. It is a lookup in Fig. 28. Note that 0 means that the beam separation is smaller than 12-15 mm (to be ignored). Please note that *m_dma* and *m_bs* are needed for the final calculations into MAD-X.

- Next comes the vector represented by 6 columns with names starting with *ma_* for displacement of cryostats.

- The last column *error detail* allows to reconstruct how the geometry imperfection was generated, and which were the assumptions on the uncertainties.

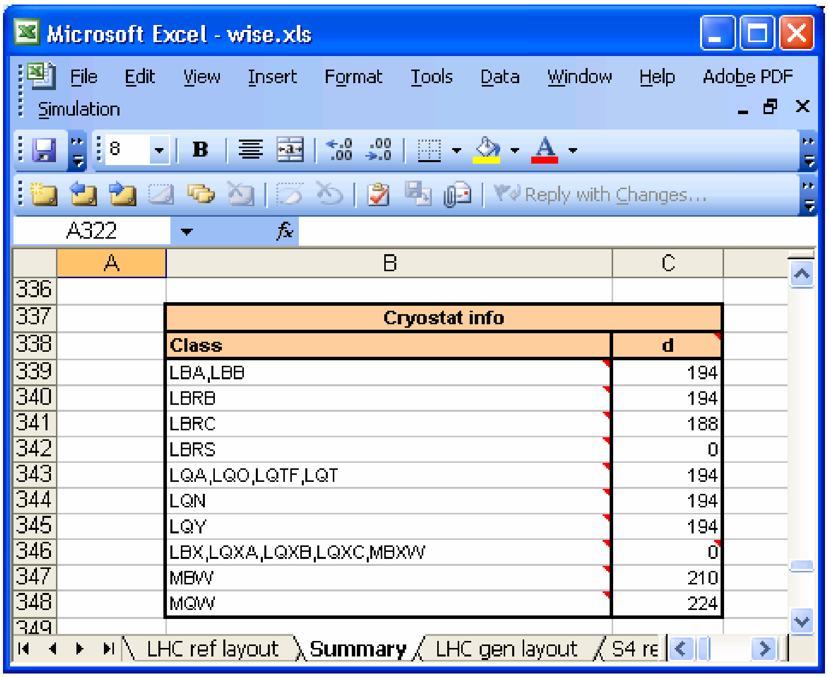


| Cryostat info | |
|---|---|
| **Class** | **d** |
| LBA,LBB | 194 |
| LBRB | 194 |
| LBRC | 188 |
| LBRS | 0 |
| LQA,LQO,LQTF,LQT | 194 |
| LQN | 194 |
| LQY | 194 |
| LBX,LQXA,LQXB,LQXC,MBXW | 0 |
| MBW | 210 |
| MQW | 224 |

Fig. 28. Table in *Summary* sheet used for lookup of beam separation (d)

# 5. THE LHC LAYOUT AND SLOT ALLOCATION

The WISE simulation needs to have the layout of the LHC machine in order to know which magnets to produce errors for. It also needs to know some derived data. The sheet *LHC ref layout* contains this information. It also contains the actual slot allocation, both official and pre-allocated by project engineers. This constitutes known information about LHC layout. The slot allocation is updated manually as described in section 2.

In order to complete (build) the entire machine, WISE needs to assign magnets to empty slots using realistic values for the magnets. In order to separate facts from simulation, WISE copies the sheet *LHC ref layout* to *LHC gen layout* (generated layout) and completes the slot allocation in this sheet. Therefore this is the sheet used during the actual simulation. The actual work of completing the slot allocation involves access to databases and derived information in other sheets inside WISE.

## 5.1 The sheet *LHC ref layout*

The WISE simulation loops sequentially over the information in the sheet *LHC ref layout* from first to last row. Fig. 29 shows the first rows in the sheet. Since it contains many columns we have to show it as two separate slices.

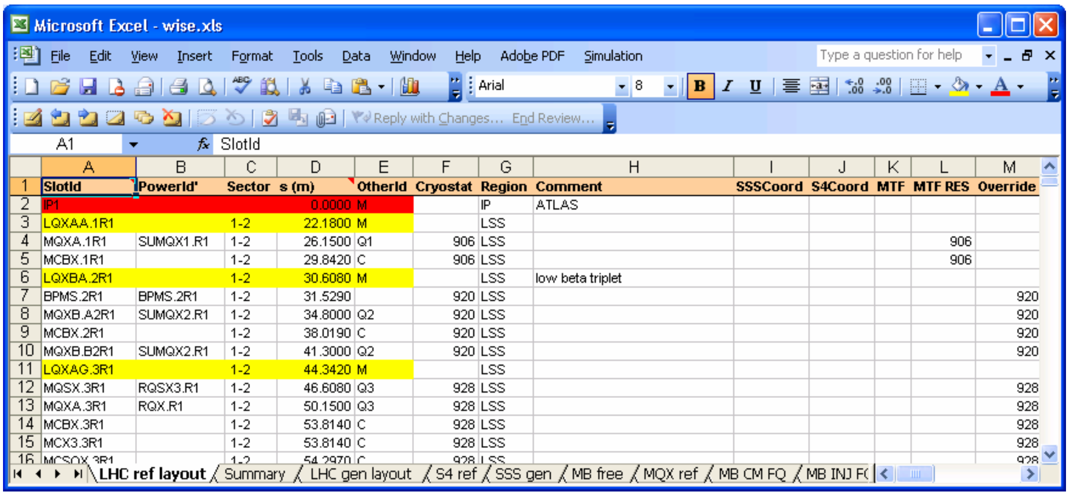

| | SlotId | PowerId' | Sector | s (m) | OtherId | Cryostat | Region | Comment | SSSCoord | S4Coord | MTF | MTF RES | Override |
|---|---|---|---|---|---|---|---|---|---|---|---|---|---|
| 2 | IP1 | | | 0.0000 | M | | IP | ATLAS | | | | | |
| 3 | LQXAA.1R1 | | 1-2 | 22.1800 | M | | LSS | | | | | | |
| 4 | MQXA.1R1 | SUMQX1.R1 | 1-2 | 26.1500 | Q1 | 906 | LSS | | | | | 906 | |
| 5 | MCBX.1R1 | | 1-2 | 29.8420 | C | 906 | LSS | | | | | 906 | |
| 6 | LQXBA.2R1 | | 1-2 | 30.6080 | M | | LSS | low beta triplet | | | | | |
| 7 | BPMS.2R1 | BPMS.2R1 | 1-2 | 31.5290 | | 920 | LSS | | | | | | 920 |
| 8 | MQXB.A2R1 | SUMQX2.R1 | 1-2 | 34.8000 | Q2 | 920 | LSS | | | | | | 920 |
| 9 | MCBX.2R1 | | 1-2 | 38.0190 | C | 920 | LSS | | | | | | 920 |
| 10 | MQXB.B2R1 | SUMQX2.R1 | 1-2 | 41.3000 | Q2 | 920 | LSS | | | | | | 920 |
| 11 | LQXAG.3R1 | | 1-2 | 44.3420 | M | | LSS | | | | | | |
| 12 | MQSX.3R1 | RQSX3.R1 | 1-2 | 46.6080 | Q3 | 928 | LSS | | | | | | 928 |
| 13 | MQXA.3R1 | RQX.R1 | 1-2 | 50.1500 | Q3 | 928 | LSS | | | | | | 928 |
| 14 | MCBX.3R1 | | 1-2 | 53.8140 | C | 928 | LSS | | | | | | 928 |
| 15 | MCX3.3R1 | | 1-2 | 53.8140 | C | 928 | LSS | | | | | | 928 |
| 16 | MCSOX.3R1 | | 1-2 | 54.2970 | C | 928 | LSS | | | | | | 928 |

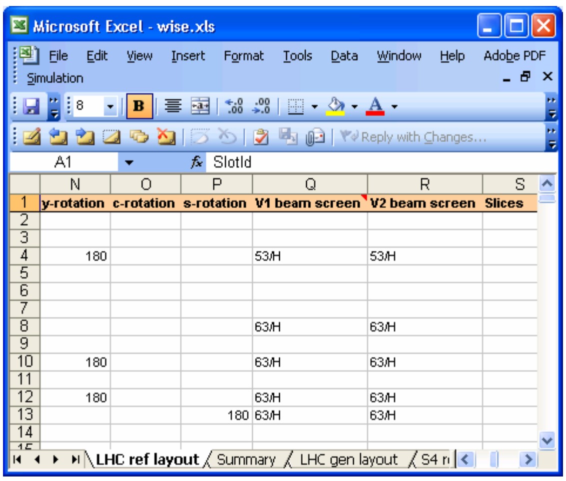

| | y-rotation | c-rotation | s-rotation | V1 beam screen | V2 beam screen | Slices |
|---|---|---|---|---|---|---|
| 2 | | | | | | |
| 3 | | | | | | |
| 4 | 180 | | | 53/H | 53/H | |
| 5 | | | | | | |
| 6 | | | | | | |
| 7 | | | | | | |
| 8 | | | | 63/H | 63/H | |
| 9 | | | | | | |
| 10 | 180 | | | 63/H | 63/H | |
| 11 | | | | | | |
| 12 | 180 | | | 63/H | 63/H | |
| 13 | | | 180 | 63/H | 63/H | |
| 14 | | | | | | |

Fig. 29. The first rows in the sheet *LHC ref layout*

The optics sequence is described in increasing *s*-coordinate corresponding to beam 1. See column *s (m)*. The optics sequence of beam 2 is so similar that we only use one sequence for simulation. The corresponding s-coordinate of beam 2 can be found from

$$s_2 = l_{lhc} - s_1 \tag{13}$$

Beam 1 starts in the ATLAS cavern and travels towards the Jura mountains and bends around Pays-de-Gex. Fig. 30 shows the ring layout.

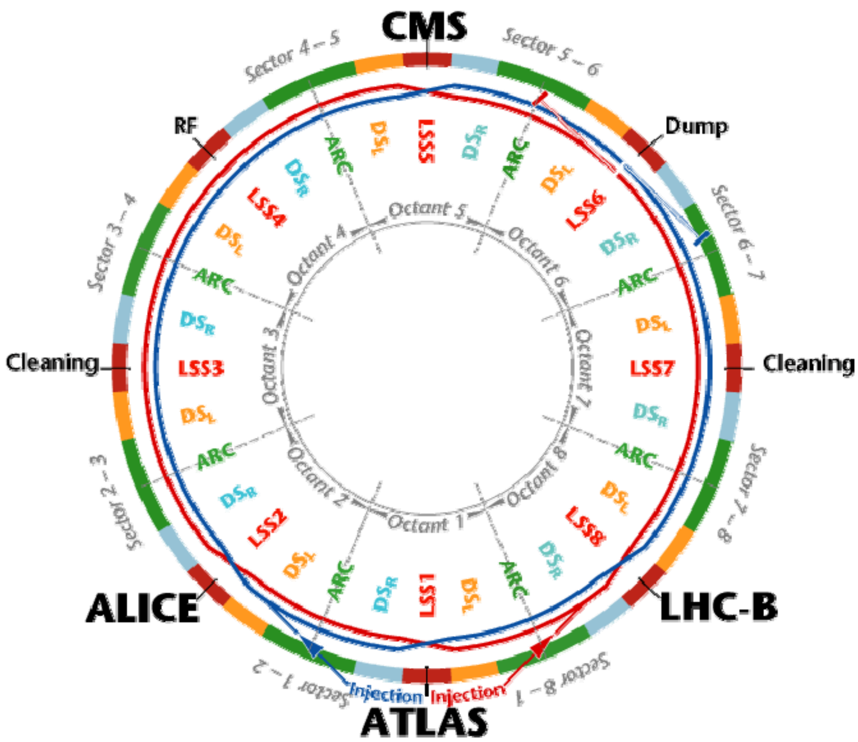


Fig. 30. The *LHC ring* with definitions of sectors, octants, and 8 IPs (4 experiments, 4 insertion regions)

The columns *Sector* and R*egion* in the sheet come from the definitions in Fig. 30. The columns *Vn* beam screen is used for magnets not having the default beam screen. The *Slices* column is the number of slices used in the LHC thin lens optics files. The column *y-rotation* contains the value 180 if an optical element has been π-rotated around the vertical axis during assembly into cryostat, or if the cryostat has been π-rotated inside the tunnel. Information about cryostat rotations are needed when estimating geometry errors.

The sheet *LHC ref layout* was made to contain a subset of optical MAD-X elements. This is sufficient for the magnetic field errors. When the geometry errors were added, the need for describing cryostats or magnet assemblies came along. This was done by merging some information from the LHC layout database [14] with the optical sequence already present in WISE. This part of the *LHC ref layout* is manually updated using some simple Excel macros external to WISE. Since the subset of info used in WISE does not change frequently it is a reasonable but not ideal approach.

Let us take a look at one cryostat in order to understand how to interpret the remaining bulk of information in the *LHC ref layout* sheet. Fig. 31 shows one cryostat that demonstrates most features.

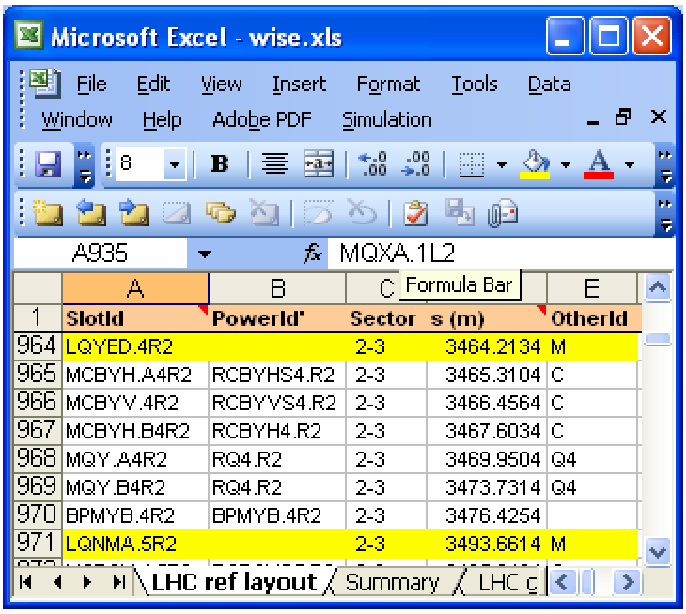


Fig. 31. The element sequence for a cryostat in the sheet *LHC ref layout*

- *OtherId* contains information about how to interpret the row. It acts like a type tag for *SlotId*.
  - If *OtherId* has the value *M* it is a marker. The concept of markers is well-known from MAD-X. In Fig. 31 it has been used twice. The first marks the beginning of the cryostat. The second marker is the beginning of the next cryostat. In-between we find the sequence of optical elements. The *SlotId* for the markers starts with *L*. See [2] for equipment codes. The second letter gives the main optical function of the cryostat; *Q* for (de)focusing quads, *B* for bending dipoles, and so forth. Another use of markers in WISE is for the IPs.
  - If *OtherId* has the value C it is a corrector magnet.
  - If *OtherId* equals *Qnn* it is a main quadrupole in the cryostat. In Fig. 31 we see two of them. If we take *OtherId* and add the 2 last characters from *SlotId* we get the functional optical identifier for the main magnet. For example *Q4.R1* which means that it is the $4^{th}$ quadrupole from the right side of IP1. In Fig. 31 we see furthermore that *Q4.R1* consists of 2 distinct MQY magnets.
  - If *OtherId* equals D*n* it is a main dipole magnet in the insertion region.
  - If *OtherId* starts with *LB* it is the equipment code of the corresponding cryostat. The reason WISE uses is a bit historic. This is the notation commonly used by the Dipole Coordination [15] which is one source of information used by WISE.
  - The *OtherId* is empty for elements used for monitoring. The monitoring equipment was added in the WISE sequence for the purpose of simulating observation errors in instruments.
- *SlotId* contains the name of the optical magnetic element as defined by LHC optics files. Note that in WISE since we dropped the beam suffix present in MAD-X.
- *PowerId* contains the functional name of the power supply for the magnet. Like for the *SlotId*, the beam suffix is missing.
- *Cryostat* contains the cryostat number if a cryostat or magnet assembly has been assigned.

- *CryoStat* is generated from the columns *SSSCoord, S4Coord, MTF, MTF Res, Override.* This takes place when using the menu choice *Update LHC slot allocations …* in Fig. 2. *SSSCoord* and *S4Coord* are pre-allocations made by the magnet coordinators for quadrupoles in arc and insertion regions. You fill find URLs to this information from [15]. WISE reads this information directly via the file system and the web. The *MTF* and *MTF Res* are two different database queries accessing the MTF [10] databases based upon decisions by MEB [16]. The columns report equipment installed or reserved for a functional slot. *CryoStat* is updated if at least one information source has an allocation. If the different information sources disagree it is considered an error and the *CryoStat* column is not updated.

- *Override* is reserved for the user of WISE. This column allows you to specify a cryostat id of your own choice. This is foreseen for *what if* scenarios when you want something different than already foreseen and you do not want WISE to impose a random choice. WISE will not check for any consistency if *Override* is used (whether magnet is free for use or that it is supposed to exist).

- The cryostat numbering space goes as follows:

  - *001-4xx.* MQ cryostats in arcs

  - *501*-532. MQ cryostats in dispersion suppressors and insertions

  - *601-7xx.* Special quadrupoles (MQM, MQY, MQTL) in insertions

  - *901-94x.* Inner triplet quadrupoles *(MQX)* around the experimental IPs

  - *1001-3xxx.* Main bending dipoles (MB) in arcs

- The cryostat numbering of inner triplets is invented by WISE. The reason is that the full breakdown structure is not available in MTF. That is, what magnets are inside the triplets cannot be deduced from a database query at present. To avoid any confusion, we have introduced a small range in WISE for these magnets. The sheet *MQX ref* contains the definition of the inner triplets. This is needed for mapping cryostats to magnets and magnetic field measurements.

- The "warm" magnets (like *MQW)* have no cryostat. The *Cryostat* column contains the magnet number for these. Other "cold" magnets have been cryostated elsewhere (like *MBRC*). For such cases the magnet type plus the cryostat id is needed to unambiguously specify the magnet assembly in question.

### 5.2 The WISE slot allocation

WISE needs to fill all functional magnetic slots in the machine before running the simulation. It does not need to be updated before each simulation, but it can be updated once in a while, either manually or automatically as explained in section 2. We start the slot allocation by making a snapshot of the *LHC ref layout* by copying it into the sheet *LHC gen layout*. Columns not needed for simulation are omitted. Slots which are not allocated are filled with not allocated magnets (of the same type) already measured. If this is not enough to fill the machine, measurements are generated according to the statistics. This rather complex piece of code has been instrumental in being able to carry out simulations in the early stage of the allocation and installation. It gradually becomes obsolete and today the slot allocation has been completed by MEB. Therefore we will not enter the details of the code implementation.

## 6. CONCLUSION

In this report we described the code WISE whose main aim is to translate all the magnetic and geometric measurements carried out in the last 5 years into an input file of MAD-X to have the best model of the LHC. The code also includes an estimate of the uncertainties associated to the measurements. In section 2 we have shown the main features of the simulation menu and the different options.

Data are retrieved from several databases: magnetic measurements, slot allocation, geometry, lay-out. An important outcome of WISE is also the fact that all the relevant data are downloaded to a worksheet and therefore are available in a user-friendly format for validation and cross-checks. In section 3, 4 and 5 we described in detail how these data are accessible in the different worksheets.

The code has been already used for different types of simulations such as beta-beating estimates and dynamic aperture studies. At the moment, one can run the injection and the high field case. In the near future, the code will refer the magnetic part to the FiDeL model, thus being able to simulate the machine in any condition.

Like in the *Forrest Gump* movie we conclude: "…and that's all that I have to say about that!"

### Acknowledgements

We wish to acknowledge numerous colleagues in the AT and AB departments. We thank Jean-Pierre Koutchouk as the driving mentor behind this work; Ezio Todesco for help to the magnetic model, validation of the code and finally helping in preparing this report; Elena Wildner for help to geometric model, uncertainties associated to geometry, database structures, and validation of the code; Bernard Jeanneret, Dominique Missiaen for help to the geometric model, beam screens and validation of misalignment calculations; Christine Vollinger, Natalia Emelianenko, Laurent Deniau, Vittorio Remondino, Rob Wolf, Nuria Catalan Lasheras, Ranko Ostojic, Tatiana Vanenkova, Suitberg Ramberger, Didier Cornuet, Fabrice Simon, Maria Durante for providing measurement data; Stephane Sanfilippo for uncertainty estimates related to magnetic measurements; Luca Bottura for explaining formula for field rotations in 2D; Walter Venturini Delsolaro for fitting parameters for the magnetic hysteresis effects. David Widegren, Sonia Mallon Amerigo, Herve Prin for convenient access to manufacturing data of the magnets; Samy Chemli for access to the LHC layout database; Markus Zerlauth and Stephan Russenschuck for information about the powering interconnections of the magnets; Thys Risselada, Werner Herr for advice concerning MAD and implementation of support scripts; Massimo Giovannozzi, Yannis Papaphilippou, Frank Schmidt, Stephane Fartoukh for validating field quality output of WISE, using the code, debugging it, and useful advices on the implementation. We apologise for any person accidentally forgotten or disturbed by numerous unwise questions during the project.

## A. INSTALLING WISE

The WISE software tool is available via a web browser as well as from CERN NICE PCs. The web site is [http://cern.ch/wise](http://cern.ch/wise) .Here you find further instructions about access. Do not hesitate to contact the author if you have questions. Copy the following files from the WISE *Release* folder to a local folder where you will be running WISE:

*wise.xls*
*wise-template.madx*
*unix-wrapper.txt*

- You will also need to copy MAD-X support scripts and files from the *Release* subfolder *MAD-X Support* to the UNIX directory where you will be running MAD-X.
- The subfolder *MAD-X Analysis* contains some simple Excel files and macros for processing the MAD-X output.
- The *Doc* subfolder contains this project report.

## B. LHC OPTICS FILES

The root of the official LHC optics file is the AFS folder:

*/afs/cern.ch/eng/lhc/optics*

You find several versions of the optics files here, each one in a separate subfolder. The most used optics version during the development of WISE are *V6.5*, *V6.500* and *V6.501*. In particular *V6.500* was the most used one in 2006 (development version). Each version contains a complete set of optics sequence and strength files that go together. Unfortunately some naming conventions have not been adhered to rigorously so WISE has some ad-hoc logic inside to generate the correct file names for the .madx scripts. Also note that not all combinations of scenarios are supported and will result in a warning message from WISE. But the logic in WISE needs manual update as well, so one day it might happen more scenarios have been added to the LHC optics files but you cannot get WISE to accept it. In this case do not hesitate to contact the author.

The optics files are divided into *.seq* files for the sequence and position of optics elements. The sequence is generated from the LHC layout. The layout, once chosen, is time-invariant. But the LHC machine has several well-defined states for injecting, accelerating, colliding and ejecting the beam, and powering of the magnets change with time. At a given time, MAD-X only handles one of these scenarios. The .str files assign "strength" (that is: normalised field strength) to the various magnets. Each file describes one scenario. These naming conventions are used: *inj* for injection at 450 GeV, *ecol* for early collision during commissioning, *col* for collisions at 7 TeV, eion for early ions during commissioning, *ions* for lead nucleus (Pb stripped for electrons) at collision energy.

There are 2 models of the LHC machine: *thin* lens and *thick* lens. The naming convention is to use *thin* for thin lens and nothing for *thick*. Lastly, there are two beams. Beam 1 circulates clock-wise and beam 2 circulates counter-clockwise. Beam 1 is the default. The naming convention for beam 2 in the optics files is *beam_four.*

## C. RANDOM GENERATOR

The random generator is a delicate piece of code. If the periodicity or distribution of the random generator is unsuitable then we introduce some subtle software-modulation of random variables which would not be present in the real world. The random generator is based upon the *Rnd* function in Excel.

WISE has built functions around this function to cover 2 distinct needs. The 1st need was to draw one distinct object out of many (*discrete* distribution). This is used for example in the slot allocation for slots where magnet has been assigned (see section 5). The 2nd need is for drawing from *continuous* distributions.

The Gaussian random generator is built on top of the rectangular one based upon the *central limit theorem* [17]. The default in WISE is to construct a "Gaussian" value by drawing 5 times from the rectangular distribution. If the resulting value exceeds 3σ, we draw again. Tests show that increasing this number to say 10 or more does not improve the probability curve. The random generator can be seeded automatically from the internal clock (different each time) or externally by giving an integer. Sometimes we might need to reproduce a simulation with the same sequence of drawn values in a deterministic way. This is why the pseudo-random seeding option is available.

## REFERENCES

[ 1] MAD-X web page, http://www.cern.ch/mad.
[ 2] The LHC Design Report, Vol. I, CERN 2004-003 (2004), http://lhc.web.cern.ch/lhc/.
[ 3] The FiDeL web page http://cern.ch/fidel/.
[ 4] The AFS service, IT dep, http://consult.cern.ch/service/afs/.
[ 5] The LXPLUS and LXBATCH public services, IT dep, http://cern.ch/plus/.
[ 6] Estimates of b6 and b10 for MQX and MQY. AT/MTM memo 708558.
[ 7] Beam screen assignments in LHC. EDMS document 483868.
[ 8] Field Error Naming Conventions for LHC Magnets. EDMS document 90250.
[ 9] AT/MTM magnetic measurements. Web site https://sma.cern.ch
[10] MTF - Manufacturing and Test Folders. Web site https://edms.cern.ch/asbuilt/plsql/mtf.home
[11] AT/MCS measurements. Web site http://cern.ch/lhc-div-mms/MMSPAGES/MA/DB/
[12] AT/MEL magnetic measurements. Web site https://cern.ch/at-div-mel-mc-analysis/
[13] Private communication with Vittorio REMONDINO in AT/MEL.
[14] The LHC layout database behind the web site http://cern.ch/layout/
[15] Dipole Coordination web site http://cern.ch/LHC-dipcoor/
[16] MEB web site http://edms.cern.ch/lhc_proj/plsql/lhcp.page?p_number=7600
[17] Wikipedia web page, http://en.wikipedia.org/wiki/Central_limit_theorem
[18] S. Sanfilippo et al, "Transfer function of the quadrupoles and expected beta-beating", *proceedings of LHC Project Workshop XV* **CERN-AB-2006-014** (2006) 151-156.
[19] M. Giovannozzi et al, "Dynamic Aperture Studies for the CERN LHC: Comparison between statistical assignments of magnet field errors and actual measured field errors", *proceedings of EPAC06* (2006) 2128-2130.
[20] P. Hagen et al, "WISE – An Adaptive Simulation of the LHC Optics", *proceedings of EPAC06* (2006) 2248-2250.